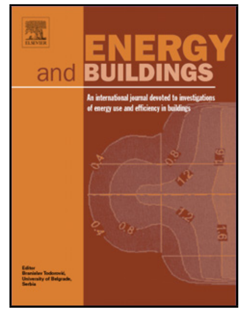

Title: Ventilation guidelines for controlling smoke, dust, droplets and waste heat: Four representative case studies in Chinese industrial buildings

Author: Yanqiu Huang Yi Wang Xiaofen Ren Yang Yang Jie Gao Yan Zou

PII: S0378-7788(16)30651-X
DOI: http://dx.doi.org/doi:10.1016/j.enbuild.2016.07.046
Reference: ENB 6877

To appear in: *ENB*

Received date: 4-4-2016
Revised date: 29-6-2016
Accepted date: 22-7-2016

Please cite this article as: Yanqiu Huang, Yi Wang, Xiaofen Ren, Yang Yang, Jie Gao, Yan Zou, Ventilation guidelines for controlling smoke, dust, droplets and waste heat: Four representative case studies in Chinese industrial buildings, Energy and Buildings http://dx.doi.org/10.1016/j.enbuild.2016.07.046

Ventilation guidelines for controlling smoke, dust, droplets and waste heat: Four representative case studies in Chinese industrial buildings

Yanqiu Huang[a], Yi Wang[a*], Xiaofen Ren[a,b], Yang Yang[a], Jie Gao[a], Yan Zou[a]

[a] *School of Environmental and Municipal Engineering, Xi'an University of Architecture and Technology, Xi'an 710055, China* [b] *Hebei University of Engineering, Hebei 056038, China*

***Corresponding Author:**

Tel: +86 029 82202729; Fax: 0086 029 82202729; Email: wangyi6920@126.com

Highlights:

- Detailed design of an exhaust hood could improve pollutant capture rates.
- Dust source characteristics are presented to guide how to reduce dust emissions.
- Movement and control of water droplets without and with ventilation are analyzed.
- Underground tunnel ventilation is energy-efficient adapting to local climates.

Nomenclature			
Ar_{exh}	Archimedes number of the exhaust duct	T_{to}	air temperature of underground tunnel outlet, K
C_{exh}	N_2O concentration of the exhaust duct at the sampling point in the local ventilation system, ppm	T_{outlet}	absolute temperature of the outlet in the general ventilation system, K
C_s	N_2O concentration of the source at the sampling point, ppm	T_s	absolute temperature of the source at the sampling point, K
D	droplets' mean diameter at computational time, μm	t	time at a specific moment, s
D_0	droplets' initial diameter, μm	V_1	push-flow velocity, m/s
d_0	diameter of the hopper outlet, mm	V_2	pull-flow velocity, m/s
$\overline{d_p}$	mean diameter of materials, μm	v_{exh}	airflow velocity of the exhaust ducts, m/s
G	ventilation rate, kg/s	v_{outlet}	airflow velocity of the outlet in the general ventilation system, m/s
L	tunnel length, m	v_{to}	tunnel outlet air velocity, m/s
L_1^*	original aspect ratio of the exhaust hood	v_s	airflow velocity of the source, m/s
L_2^*	new aspect ratio of the exhaust hood	Z	drop height, m

n	droplets number at computational time	**Greek symbols**	
n_0	droplets initial number when generating	ρ_p	density of materials, kg/m^3
P_f	relative gauge pressure of the fresh air inlet at the sampling point, Pa	ρ_b	bulk density of materials, kg/m^3
T_{exh}	absolute temperature of the exhaust duct at the sampling point, K	η_r	ratio of the quantity of PM_{10} dust emission to the quantity of the bulk materials, g/kg
T_f	absolute temperature of the fresh air inlet at the sampling point, K		

Abstract:

Four representative studies were selected to investigate industrial ventilation guidelines for controlling smoke, dust, droplets and waste heat. In the first case, exhaust hoods were designed to improve the smoke capture rates during the pouring process. It demonstrated that constructing the exhaust hoods with large aspect ratio and contain volume could improve the capture rates. The second case addresses the detailed characteristics of dust generated from bulk materials transport. The results indicated that the dust emission rate could be reduced by decreasing the drop height and the percentage of 0~10μm in the materials in the transitive regime while by decreasing the percentage of 0~10μm in the materials in the dispersive regime. The third case addresses the movement and control of water droplets from an opening tank. It showed that the droplet diameter was distributed nonuniformly without push-pull ventilation; with push-pull ventilation, the control effect increased with decreasing initial diameter. The last case focuses on a ventilation system adapted to local climates. It illustrates that there is an optimal underground tunnel

length. In summary, these conclusions offer valuable knowledge to develop high-efficiency ventilation systems with improved indoor air quality and low energy consumption for industrial buildings.

Keywords: High-efficiency ventilation system; Smoke; Dust; Droplets; Waste heat

1. Introduction

The constructed floor area of industrial buildings in China has grown rapidly and is still increasing at a steady pace [1-5]. This growth rate was over 13% from 2010 to 2011; the constructed floor area was over 500 million square meters per year since 2011 and has continued to increase (Fig. 1). A number of problems have arisen during the development of industrial buildings. One of the crucial problems is that the energy efficiency of the ventilation systems in industrial buildings is still quite low, thus leading to serious pollution and high energy consumption.

Fig. 1

There are various types of industries in China, such as metallurgy, cement, plating and casting. In industrial buildings, the most common application of ventilation systems is for the removal of the pollutants, such as smoke, dust, droplets and waste heat [6]. Scene photos of these four typical pollutants in Chinese industrial buildings are shown in Fig. 2. In most situations, there are large amounts of released gaseous and particulate pollutants and indoor high-intensity waste heat. Both the high concentration and the high temperature of pollutants in industrial buildings could harm workers' health, especially in the buildings with low energy efficiency ventilation systems. The intense pollution and overheating resulted in 29,972 cases of occupational disease in China in 2014 [7]. Therefore, occupational health and safety in industrial buildings should not be ignored.

Fig. 2

In addition, energy consumption in industrial buildings is generally high. Survey data revealed that the energy consumption of heating, air conditioning and mechanical ventilation systems in Chinese industrial buildings accounts for 80-90% of their total energy consumption. For most industrial plants, the efficiency of the ventilation system is still quite low, leading to the rapid increase of building energy consumption. Thus, environmental improvement through improving the energy efficiency of ventilation systems is an urgent task for further development of the industries in China.

Ventilation guidelines for controlling smoke, dust, droplets and waste heat could be disclosed with the help of advanced experimental instruments and simulation methods. Detailed flow information about smoke, dust and waste heat can be achieved through advanced experimental instruments, such as a Laser Doppler Anemometer (LDA) [8-9], a high speed camera [10-12], Particle Image Velocimetry (PIV) [13-15] and a three-dimensional hot bulb anemometer. Additionally, estimating the whole flow evolution information of smoke and droplets [16-18] and designing an energy-efficient ventilation strategy that takes advantage of the local climate to control waste heat can be obtained by precise numerical simulation [19-20] with the development of the grid generation method [21-22], the turbulence model [23], the solution strategy, etc.

Removing or controlling of smoke, dust, droplets and waste heat are typical objects in designing an industrial building. This study aims to provide ventilation guidelines for controlling these pollutants efficiently by examining four representative case studies in Chinese industrial buildings. Advanced experimental instruments and simulation methods were adopted based on different features of these four cases. The conclusions obtained could help develop a high-efficiency ventilation system to improve indoor air quality and save energy consumption in industrial buildings.

2. Study of representative cases for controlling four pollutants

Four representative cases were selected to investigate the ventilation guidelines for controlling smoke, dust, droplets and waste heat in industrial buildings. The first case study, i.e., smoke control, was the most comprehensive and mainly consisted of three parts. First, the empirical factors for designing an exhaust hood to improve the smoke capture rates were investigated experimentally. Then, the evolution of the escaped smoke distribution was exhibited to indirectly reflect the hood performance using numerical simulation. Finally, the obtained results were successfully applied to a renovation project according to field measurements. The second case, i.e., dust control of gas-solid two-phase flow, focused on experimentally determining the flow regimes and dust emission rates of three materials in a free falling particle stream. Compared to the study of dust control, the third case, i.e., droplet control of gas-liquid two-phase flow, focused on the evaporation and motion characteristics of water droplets and the influencing factors of the push-pull ventilation system on capturing water droplets using numerical simulation. The last case, i.e., waste heat control by taking advantage of the complex local climate, focused on the distribution of indoor air temperature and velocity using field measurements and determining the influencing factors on the cooling capacity of an underground tunnel using numerical simulation. To summarize, the analysis of the four representative cases could help develop a high-efficiency ventilation system to improve indoor air quality and reduce energy consumption in industrial buildings. The detailed studies are introduced in the following four sections.

2.1 Detailed design of an exhaust hood to capture high-temperature smoke

In some industries, such as metallurgy and casting, high-temperature smoke is the main cause of heavy pollution of occupied zones in large plants. The current ventilation system is usually ineffective because the exhaust hood cannot be installed above the heat source due to production process restrictions. This case illustrates how to design an exhaust hood to improve the capture rates of high-temperature smoke during the pouring process in steel plants. In addition, the evolution of the escaped smoke distribution was determined to indirectly reflect the performance of the exhaust hood. Furthermore, the application effect of the renovation project was demonstrated based on the obtained research results. First, the aspect ratio of the exhaust hoods was experimentally investigated when the source was assumed to be constant. Then, the exhaust hoods' volume was experimentally investigated when the source was assumed to be intermittent.

Our previous paper [8] described the experimental facilities and instrumentation in detail, so only a synopsis is provided here. The experimental setup shown in Fig. 3 consisted of a supply air system, exhaust system and measurement system. The supply air system consisted of both mechanical and natural supply air. The exhaust system mainly included local exhaust hoods, general ventilation outlets and exhaust fans. The measurement system mainly included velocity, temperature and tracer gas (N_2O) concentration measurement systems. Multi-Gas Monitor Type 1303 and Multi-Sampler and Doser Type 1412 were adopted to determine the tracer gas concentration. Two tubes were used for sampling the air in the exhaust ducts.

Fig. 3

Capture efficiency has been widely used to evaluate exhaust systems for controlling steady-state pollutants. The higher the capture efficiency is, the higher the capture rate of the smoke is. Fig. 4 indicates the relationship between the capture efficiency and the Archimedes number of the exhaust duct (Arexh) influenced by two exhaust hood aspect ratios.

Fig. 4

Fig. 4 shows that the capture efficiency varied linearly if the lg-grid was used on the horizontal axis ($-1.0 < lgAr_{exh} < 1.0$). The slopes of the lines were approximately the same, but the intercepts differed greatly with different aspect ratios. Quantitatively, the capture efficiency decreased by 5% if the aspect ratio was reduced from 6 to 3. Therefore, from the view of pollutant control, it would be beneficial to construct the largest exhaust hood aspect ratio as practically possible to form a large hood opening.

The smoke generated during the pouring process was characterized by huge, instantaneous emissions that continuously changed with time. Therefore, it is better to assume that the smoke is an intermittent source to make the experimental results more precise. A larger volume exhaust hood was proposed by enlarging the hood volume in the hood height direction to avoid impacting the pouring process. The experimental results showed that enlarging the hood volume may dramatically improve the cumulative smoke capture rates. The reason for this is probably that the buffer space formed by the enlarged volume could provide peak shaving, meaning that smoke was contained inside the exhaust hood for some time before it was removed. Overall, it is feasible to use an exhaust hood with a larger contain volume to improve the cumulative pollutant capture rates during the whole pouring process.

In addition to the smoke capture rates, the performance of the exhaust hood could also be evaluated by the evolution of the escaped smoke distribution in the space. The tracer gas, i.e., N_2O, was used to simulate smoke. The evolution of the escaped N_2O concentration distribution in the space was determined using a numerical simulation that was validated by the experimental measurements.

Using the same parameters as the previous experiments from [8], a validation model was built to support the reliability of the simulation. For the mesh, local refinement and Tetrahedral/Hybrid mesh elements were adopted to discretize the domain. A grid with 4,820,000 cells was chosen based on the grid sensitivity analysis. The set of simulation boundary conditions was derived from the experimental measurements, and the details are shown in Table 1.

Table 1

The realizable k-ε turbulence model was used to achieve a three-dimensional airflow-field. The standard wall function was adopted for near-wall treatment, and 0.1 s was selected as the time step to obtain the unsteady concentration field. Compared with the experimental data from [8], the validation of the simulation results based on the N_2O concentration of the exhaust duct is shown in Fig. 5.

Fig. 5

Fig. 5 shows that the variations of exhaust duct N_2O concentration between the simulations and experiments were consistent. In addition, the average deviation of the N_2O concentration between them was 19.46%. To summarize, the validation confirmed the accuracy of the numerical simulations for the unsteady spatial distribution of pollutant concentrations.

The evolution of the escaped N_2O concentration distribution in the space with time (t) is shown in Fig. 6.

Fig. 6

Fig. 6 shows that from t = 6 s, the N_2O began to accumulate in the corner. At t = 30 s, some N_2O began to escape from the exhaust hood to the upper space. The N_2O concentration distribution reached concentration stratification at t = 90 s, and it almost reached steady state at t = 240 s. Therefore, if the hood performance is desirable, the time of the N_2O escape and concentration stratification formation will be delayed, and the region of N_2O escape will decrease. In summary, it would be better for workers to operate neither during the period nor in the region of high pollutant concentrations.

The design recommendations for an exhaust hood obtained from the previous experimental measurements and numerical simulations were conducted successfully on a renovation project in a steel plant in China. Field measurements showed that the capture efficiency increased by 15% while the energy consumption of the ventilation system remained unchanged. Moreover, the dust concentrations in occupied zones were all lower than the exposure limits of 8 mg/Nm^3 [24]. In summary, satisfactory pollutant control and desirable indoor air quality could be achieved with a small exhaust hood flow rate if the hood design could take practical complex factors into account.

2.2 Micro-analysis of dust source characteristics

In many industries, such as cement and metallurgy, dust emissions are generated during the fall and impact of bulk materials transport [25]. Compared to the study of high-temperature smoke， the second case study addresses the characteristics of isothermal gas-solid flow, i.e., the detailed characteristics of dust sources generated during a falling stream of bulk materials. To reduce dust emissions and provide guidance for ventilation system design, a quantitative description of free falling particle flow is presented.

A detail description of the experimental facilities and instruments can be found in our previously published work [25]. Here, we give only a brief introduction. An experimental rig was designed to measure the dust emission quantity in the process of free fall subjected to different outlet diameters and drop heights. As shown in Fig. 7, there were three primary components of the test rig: the silo and hopper arrangement, with outlet dimensions of 2 mm, 4 mm or 6 mm, the test enclosure, which had a square cross section with a 5-cm-diameter aperture and a height from 88 cm to 148 cm, and the dust collection system. An 8-grade cascade aerosol sampler was used to measure the dust quantity. In addition to what is shown in Fig. 7, the stream characteristic was tracked by a high-speed camera (Phantom V9.1). A summary of the materials used is shown in Table 2. The experiment used 100 g materials with zero moisture content. Each experiment was repeated three times.

Fig. 7

Table 2

The experimental results illustrated that the free falling particle stream could be successively divided into a stable regime, which occurred from the hopper outlet to the first visible rupture position of the particle stream, a transitive regime, which occurred from the position of the first rupture point to the point where the cluster completely disappeared, and a dispersive regime, which occurred after the complete disappearance of the clusters (Fig. 8 (a)). The flow characteristics were similar to the results of [26-27]. In this part, the stable regime was not involved. In the test measurement range, the particle stream was in the dispersive regime when the diameter of the hopper outlet was d_0=2 mm, and the particle stream was in the transitive regime when $d_0 \geq 4$ mm, according to the results obtained by the high speed camera.

In this paper, η_r is defined as the ratio of the quantity of the PM10 dust emission to the quantity of the bulk materials present in each test. Fig. 8 (b) shows the variations of η_r for three materials versus drop height (Z) at different hopper outlet diameters.

Fig. 8

As shown in Fig. 8 (b), when $d_0 \geq 4$ mm (in the transitive regime), the ηr of each material increased with increasing drop height, and ηr, SiO_2 > ηr, AlF_3 > ηr, Al_2O_3. Combining Table 2 and Fig. 8 (b), the percentage of 0~10 μm particles in the materials and the drop height significantly contributed to the variability of the results. When d_0 = 2 mm (in the dispersive regime), the ηr of each material was approximately constant with increasing drop height, and ηr, SiO_2 > ηr, AlF_3 > ηr, Al_2O_3. Therefore, the percentage of 0~10 μm particles in the materials was important for the dust emission rate, but the drop height was not. By comparing the dust emission rate of the three materials in the above two flow regimes, it was found that the dust emission rate of SiO_2 was approximately 1.19 to 2.9 times that of AlF_3 and 4.18 to 6.54 times that of Al_2O_3. Thus, the percentage of 0~10 μm particles in the materials mainly accounted for the dust emission rate although the flow regime differed. Accordingly, dust emissions could be reduced by minimizing either the percentage of 0~10 μm particles in the materials or the drop height when the particle stream is in the transitive regime; it could also be reduced by minimizing the percentage of 0~10 μm particles in the materials when the particle stream is in the dispersive regime.

2.3 Evaporation and motion characteristics of droplets

Water or acidic droplets in industrial buildings may harm workers' health [28-29] and the indoor environment and negatively affect the building's durability [30]. Different from the study of gas-solid flow in case 2 due to evaporation, the third case study addresses the motion characteristics of gas-liquid flow, i.e., water droplets and the influencing factors of the local ventilation system. In this part, numerical simulation using a Lagrangian-Eulerian approach [31-32] was adopted to study the evaporation and movement of monodispersed water droplet populations generated from an opening tank during industrial production processes and the control effects of a push-pull ventilation system. A typical push-pull ventilation system comprises a push nozzle and an exhaust hood that are placed on each side of an opening tank. The pollutants generated from the tank move with the aid of the push jet flow toward the exhaust hood and are thus removed. Moreover, whether the flow field has push-pull flow depends on whether the push nozzle and the exhaust hood work.

The flow rate ratio method was exploited to calculate the relevant parameters involved in the push-pull system. The length-width ratio of both the push nozzle and the exhaust hood was greater than 40; according to Li [33], airflow changes in the length direction of the slot can be neglected. Therefore, a two-dimensional geometric model was used, as shown in Fig. 9. The push nozzle and the exhaust hood were placed on the tank upper surface to form the entire push-pull system. Saturated airflow with droplets was released into the flow field. For the mesh, local refinement and triangular elements were adopted to discretize the domain. The total grid number was 193,558, and the maximum cell skewness was 0.41. Moreover, the boundary conditions of the push nozzle, exhaust hood and emissions side were set as velocity-inlet types, the left lateral side was set as a pressure-inlet type, the right lateral side was set as a pressure-outlet type, and the other was set as a wall type. Moreover, the RNG k-ε model and randomly walking model were used to separately simulate the turbulence and droplet spreading due to turbulence. The governing equations of the evaporative droplets can be found in the literature [34]. The grid-sensitivity analysis and model validation were performed in our previous research [35], so they are not repeated here.

Fig. 9

Taking droplets with an initial diameter D_0 of 20 μm for example, Fig. 10 shows the characteristics of droplet movement and evaporation when both the push nozzle and the exhaust hood did not work. Fig. 10 (a) qualitatively describes the evolution of the droplets. Under the effect of rising airflow, the droplets persistently moved upward, which could harm the working environment. Furthermore, when t=8 s and t=15 s, the diameter of the droplets in the regions close to the centreline of the tank were larger than those further away from the centreline.

Fig. 10 (b) quantitatively depicts the variations of the droplets' mean diameter (D) over time. It shows that the droplet diameter decreased slightly at first and then rapidly decreased over time; the critical time was approximately 13 s. This tendency can be explained by smaller droplets evaporating faster [36]. In particular, as droplets began to evaporate, the diameter accordingly decreased. The reduced size in turn led to a faster evaporation rate, thus causing the droplet diameter to decrease rapidly.

Combining Fig. 10 (a) and Fig. 10 (b), after being released, the droplets persistently moved upward until they totally evaporated, thus polluting the environment. It would be appropriate for workers to avoid either the droplet moving region or the period when the droplets move. Surely it would be better to control the droplets from the source considering the actual process operation.

Fig. 10

Taking droplets with D_0= 20 μm and D_0=100 μm as examples, Fig. 11 compares the evolution of droplets at four moments in the flow field with and without push-pull flow. Push-pull ventilation was obviously an effective way to remove droplets released from an opening tank. The comparison shows that when there was push-pull flow with a push-flow velocity V_1 of 0.77 m/s and a pull-flow velocity V_2 of 2.0 m/s, the flow field could form a complete air closure, and droplets were unlikely to disperse into the environment and most were captured by the hood. Furthermore, as shown in Fig. 11 (b), droplets with D_0=20 μm moved higher than droplets with D_0=100 μm due to the effects of gravity. Moreover, some droplets with D_0=100 μm fell back into the tank after release; accordingly, the number of droplets captured by the exhaust hood was less than that of droplets with D_0=20 μm.

Fig. 11 (c) shows the droplets' number change in the flow field with a push-flow velocity V_1 of 0.77 m/s and a pull-flow velocity V_2 of 2.0 m/s; in this figure, the Y-axis, n/n_0, is the ratio of the droplet number at computational time to the total number when the droplets were initially released. This figure shows that the droplets' residence time lengthened as the droplet initial diameter increased. For droplets with D_0=20 μm, all of the droplets were removed by the exhaust hood at approximately 2.1 s, whereas for D_0=100 μm, the droplets completely disappeared at approximately 9.0 s. The expel rate of droplets with D_0=20 μm was 4.5 times larger than those with D_0=100 μm.

Fig. 11

Therefore, if a complete air closure existed in the flow field, the push-pull ventilation system could remove droplets timely and efficiently, thus weakening their impacts on the working zone. Moreover, both droplet movement characteristics and the control effects were influenced by the droplets' initial diameter. Taking some measures in practice to minimize the droplet initial diameter would be conducive to controlling the droplets with a proper ventilation system.

2.4 Underground tunnel ventilation to eliminate waste heat

The utilization of geothermal energy to reduce heating and cooling needs has received increasing attention recently. Underground ventilation systems, which utilize the lower temperature of deep soil to cool outdoor air and then supply this cooled air to the building at floor level (Fig. 12), are an effective energy saving technology for buildings. In some industrial buildings with high-temperature heat sources, the indoor air temperature is usually high. So, different from the foregoing three cases, the last case, i.e., waste heat control, addresses a high-efficiency ventilation system that takes into account the complex local climate to eliminate waste heat effectively and reduce air temperature [37] in the occupied zone. In China, there are five climatic regions. The use of underground ventilation is suitable for regions with a wide annual temperature range and low underground water levels. As an energy-efficient ventilation strategy, underground tunnel ventilation is an economical and simple way to conserve energy.

Fig. 12

This case examined a large industrial plant that adopted an underground tunnel ventilation system in China. Field measurements were performed, and the following measurements were carried out: the air temperature and velocity inside the building and the air temperature and velocity at the tunnel outlet were recorded using a Swema 03 sensor (accuracy: ±0.01 m/s and ±0.5℃); the surface temperature of the heat source, the internal surface temperature of the building envelope and the underground tunnel were recorded using an infrared thermometer (±0.1℃ ±1% of the reading). A CFD prediction model for the tunnel natural ventilation system was established considering the buoyancy effect. The measured data were set as the boundary conditions. The realizable k-ε model was adopted to simulate the ventilation flow in the tunnel. Based on the Boussinesq approximation, the SIMPLE algorithm was used for the pressure-velocity coupling, and the standard wall function was used to describe the wall-bounded turbulence. After the grid-sensitivity analysis, a grid with 3,970,000 cells was chosen to balance computation time and accuracy.

Fig. 13

Fig. 13 shows that the simulated data were consistent with the data measured along the tunnel; the average deviations of air temperature and velocity were 0.68% and 5.6%, respectively. The effects of tunnel length on the outlet air temperature and the ventilation rate in the tunnel are shown in Fig. 14.

Fig. 14

As shown in Fig. 14 (a) and (b), the tunnel outlet air temperature and ventilation rate varied greatly with tunnel length. For lengths of 60 m to 200 m, the outlet air temperature decreased linearly. For lengths of 200 m to 300 m, the air temperature was approximately constant. In addition, with increasing tunnel length, the ventilation rate increased linearly and reached its highest value of 18.7 kg/s when the length was 200 m; then, the ventilation rate decreased to 16.1 kg/s when the length was 300 m. Therefore, the ventilation rate decreased when the length was greater than 200 m. This was mainly because the outlet temperature remained approximately constant as the tunnel length increased, while the frictional resistance became large when the length was more than 200 m. The pressure difference between the underground tunnel inlet and outlet decreased, and thus, the ventilation rate decreased. To summarize, there is an optimal underground tunnel length to improve the thermal environment and reduce the total energy consumption of industrial buildings with intense heat sources in certain climates.

3. Conclusions

Four representative cases were selected from Chinese industrial buildings to investigate ventilation guidelines for controlling smoke, dust, droplets and waste heat. The primary conclusions could be drawn as follows:

(1) Empirical factors (the hood aspect ratio and the hood volume) for designing an exhaust hood to improve smoke capture rates during the pouring process in steel plants were investigated. The capture efficiency decreased 5% when the hood aspect ratio was reduced from 6 to 3. Enlarging the hood volume to form a buffer space could dramatically improve the cumulative smoke capture rates. Meanwhile, the evolution of the escaped N_2O concentration distribution could indirectly reflect the hood performance. The N_2O began to escape from the exhaust hood to the ambient at t = 30 s and reached concentration stratification at t = 90 s. In summary, from the view of pollutant control, it would be beneficial to construct the largest aspect ratio and contain volume as practically possible to improve pollutant capture rates.

(2) A micro-analysis of dust source characteristics generated during the falling stream of bulk materials could offer guidelines to reduce dust emissions and capture dust efficiently. A free falling particle stream could be successively divided into three regimes, and the dust emission rate could be reduced by decreasing two parameters in different regimes. In the transitive regime, the drop height and the percentage of 0~10 μm particles in the materials should be decreased; in the dispersive regime, the percentage of 0~10 μm particles in the materials should be decreased.

(3) After generation, the distribution of the droplet diameter gradually became nonuniform. Meanwhile, the droplet diameter decreased with time slowly at first and then sharply when the droplets began to evaporate. Moreover, droplets with an initial diameter of 20 μm moved higher and were captured more by the exhaust hood than those with an initial diameter at 100 μm when in a push-pull flow filed.

Furthermore, decreasing the initial diameter shortened the droplet residence time in the flow field and thus contributed to improving the droplet control effect with a proper ventilation system.

(4) As the tunnel length increased from 60 m to 200 m, the underground tunnel outlet air temperature decreased, and the ventilation rate increased linearly; as the tunnel length increased from 200 m to 300 m, the outlet air temperature was approximately constant, and the ventilation rate decreased. Therefore, there is an optimal underground tunnel length to improve the thermal environment and reduce the total energy consumption of buildings, especially for large plants with intense heat sources under certain climatic conditions.

In summary, the conclusions obtained from the case studies representing typical pollutants in industrial buildings could help develop a high-efficiency ventilation system to improve indoor air quality and reduce energy consumption.

Acknowledgments

This research was financially sponsored by the Key Project of the National Natural Science Foundation of China (No. 51238010), the National Science Fund for Distinguished Young Scholars of China (No. 51425803) and the China Postdoctoral Science Foundation (No. 2015M580823). We also wish to thank the Civil Engineering Department at Aalborg University for their kind help and support in successfully conducting the reduced-scale experiment for high-temperature smoke.

References

1. National Bureau of Statistics of the People's Republic of China (2010) China Statistical Yearbook. China Statistics Press, Beijing (in Chinese)

2. National Bureau of Statistics of the People's Republic of China (2011) China Statistical Yearbook. China Statistics Press, Beijing (in Chinese)

3. National Bureau of Statistics of the People's Republic of China (2012) China Statistical Yearbook. China Statistics Press, Beijing (in Chinese)

4. National Bureau of Statistics of the People's Republic of China (2013) China Statistical Yearbook. China Statistics Press, Beijing (in Chinese)

5. National Bureau of Statistics of the People's Republic of China (2014) China Statistical Yearbook. China Statistics Press, Beijing (in Chinese)

6. Dallavalle JM (1952) Exhaust hoods. The Industrial Press, New York

7. Disease Prevention and Control Bureau of National Health and Family Planning Commission of the People's Republic of China (2014) Notification of occupational disease prevention in 2014.

8. Huang YQ, Wang Y, Liu L et al (2015) Reduced-scale experimental investigation on ventilation performance of a local exhaust hood in an industrial plant. Build and Environ 85:94-103

9. Fischer A, Pfister T, Czarske J (2010) Derivation and comparison of fundamental uncertainty limits for laser-two-focus velocimetry, laser Doppler anemometry and Doppler global velocimetry. Measurement 43:1556-1574

10. Royer JR, Evans DJ, Loreto O et al (2009) High-speed tracking of rupture and clustering in freely falling granular streams. Nat 459:1110-1113

11. Waitukaitis SR, Grutjen HF, Royer JR et al (2011) Droplet and cluster formation in freely falling granular streams. Phys Rev E 83:253-268

12. Esmaili AA, Donohue TJ, Wheeler CA et al (2013) A new approach for calculating the mass flow rate of entrained air in a freefalling material stream. Particul Sci Technol 31:248-255

13. Cao XD, Liu JJ, Jiang N et al (2014) Particle image velocimetry measurement of indoor airflow field: A review of the technologies and applications. Energ Buildings 69:367-380

14. Hollenbeck P (2015) The A-curve Position from an Aaberg Exhaust Hood. In: Proceedings of the 11th International Conference on Industrial Ventilation, Shanghai, 2015

15. Ansart R, Letourneau JJ, Ryck AD et al (2011) Dust emission by powder handling: Influence of the hopper outlet on the dust plume. Powder Technol 212:418-424

16. Lin CJ, Chuah YK, Liu CW (2008) A study on underground tunnel ventilation for piston effects influenced by draught relief shaft in subway system. Appl Therm Eng 28:372-379

17. Diego I, Torno S, Toraño J et al (2011) A practical use of CFD for ventilation of underground work. Tunn Underg Sp Tech 26:189-200

18. Xu G, Luxbacher KD, Ragab S et al (2013) Development of a remote analysis method for underground ventilation systems using tracer gas and CFD in a simplified laboratory apparatus. Tunn Underg Sp Tech 33:1-11

19. Sano TG, Hisao H (2012) Simulation of granular jets: Is granular flow really a perfect fluid. Phys Rev E 86:1-6

20. Zeren Z, Ansart R, Simonin O et al (2012) 3D unstationary simulations of a free-falling particle jet using a granular-kinetic hybrid mode. Ventilation:1-6

21. Bagade PM, Bhumkar YG, Sengupta TK (2014) An improved orthogonal grid generation method for

solving flows past highly cambered aerofoils with and without roughness elements. Comput Fluids 103:275-289

22. Shi X, Fang S, Lv M et al (2015) A 3D anisotropic Cartesian grid generation method and its applications in viscosity flows. Procedia Eng 99:575-580

23. Popovac M, Hanjalic K (2007) Compound wall treatment for RANS computation of complex turbulent flows and heat transfer. Flow Turbul Combust 78:177-202

24. Ministry of health of the People's Republic of China (2007) GBZ 2.1-2007 Occupational exposure limits for hazardous agents in the workplace- part 1:chemical hazardous agents (in Chinese)

25. Wang Y, Ren XF, Zhao JP (2016) Experiment study of flow regimes and dust emission in a free falling particle stream. Power Technol 292:14-22

26. Ansart R, Ryck AD, Dodds J et al (2009) Dust emission by powder handling: Comparison between numerical analysis and experimental results. Powder Technol 190:274-281

27. Möbius ME (2006) Clustering instability in a freely falling granular jet. Phys Rev E 74:121-137

28. Hyunhee P, Jang JK, Shin JA (2011) Quantitative exposure assessment of various chemical substances in a wafer fabrication industry facility. Saf Health Work 2:39-47

29. Li J, Zhou Y (2013) Occupational hazards control of hazardous substances in clean room of semiconductor manufacturing plant using CFD analysis. Toxicol Ind Health 31:123-139

30. Achenbach PR, Trechsel HR (1982) Evaluation of current guidelines of good practice for condensation control in insulated building envelopes, thermal performance of the exterior envelopes of buildings. In: Proceedings of ASHRAE/DOE Conference, Las Vegas, 1982

31. Liu L (2011) Expiratory droplet exposure between individuals in a ventilated room. Dissertation, The University of Hong Kong

32. Sun W, Ji J, Li Y (2007) Dispersion and settling characteristics of evaporating droplets in venti1ated room. Build Environ 42:1011-1017

33. Li XT, Zhao B, Shao XL et al (2011) Ventilation of Buildings. China Machine Press, Beijing (in Chinese)

34. Fluent (2006) Fluent User's Guide. ANSYS Inc, Canonsburg, PA

35. Wang Y, Zou Y, Yang Y et al (2016) Movement and control of evaporating droplets released from an open surface tank in the push-pull ventilation system. Build Simul 9:443-457

36. Xie X, Li YG, Chwang ATY et al (2007) How Far Droplets Can Move in Indoor Environments-Revisiting the Wells Evaporation-Falling Curve. Indoor air 17:211-225

37. Kumar R, Ramesh S, Kaushik SC (2003) Performance evaluation and energy conservation potential of earth-air-tunnel system coupled with non-air-conditioned building. Build Environ

List of figure captions

Fig. 1 The completed area of industrial buildings

Fig. 2 Scene photos of four typical polluants in Chinese industrial buildings

Fig. 3 Schematic diagram of the experimental setup for exhaust hoods to capture smoke: Measuring points of tracer gas concentration

Fig. 4 Capture efficiency variations of exhaust hoods with different aspect ratios

Fig. 5 Variations of exhaust duct N_2O concentration between simulations and experiments

Fig. 6 Evolution of tracer gas (N_2O) concentration (t=0~240 s) (a) *t*=0 s, (b) *t*=6 s, (c) *t*=30 s, (d) *t*=90 s, (e) *t*=240 s

Fig. 7 The experimental rig of free falling particle stream

Fig.8 (a) Schematic of dust emissions and flow regime variations during a free falling particulate stream, (b) Variations of dust emission rates

Fig.9 Geometric model with push-pull ventilation system

Fig.10 (a) Evolution of droplets (initial diameter D_0=20μm) without push-pull flow, (b) Mean diameter of droplets (initial diameter D_0=20μm) with time

Fig. 11 (a) Evolution of droplets with different initial diameter D_0 in flow field without push-pull flow, (b) Evolution of droplets with different initial diameter D_0 in flow field with push-pull system (push-flow velocity V_1=0.77 m/s, pull-flow velocity V_2=2.0 m/s), (c)Variations of droplets number in flow field with push-pull flow (push-flow velocity V_1=0.77 m/s, pull-flow velocity V_2=2.0 m/s)

Fig. 12 Schematic of the plant with underground tunnel ventilation system

Fig. 13 (a) Measured temperature profiles compared with simulated results along the tunnel, (b) Measured velocity profiles compared with simulated results along the tunnel

Fig. 14 Effects of underground tunnel length on: (a) Tunnel outlet air temperature; (b) Ventilation rate in the tunnel

Fig.1
Click here to download high resolution image

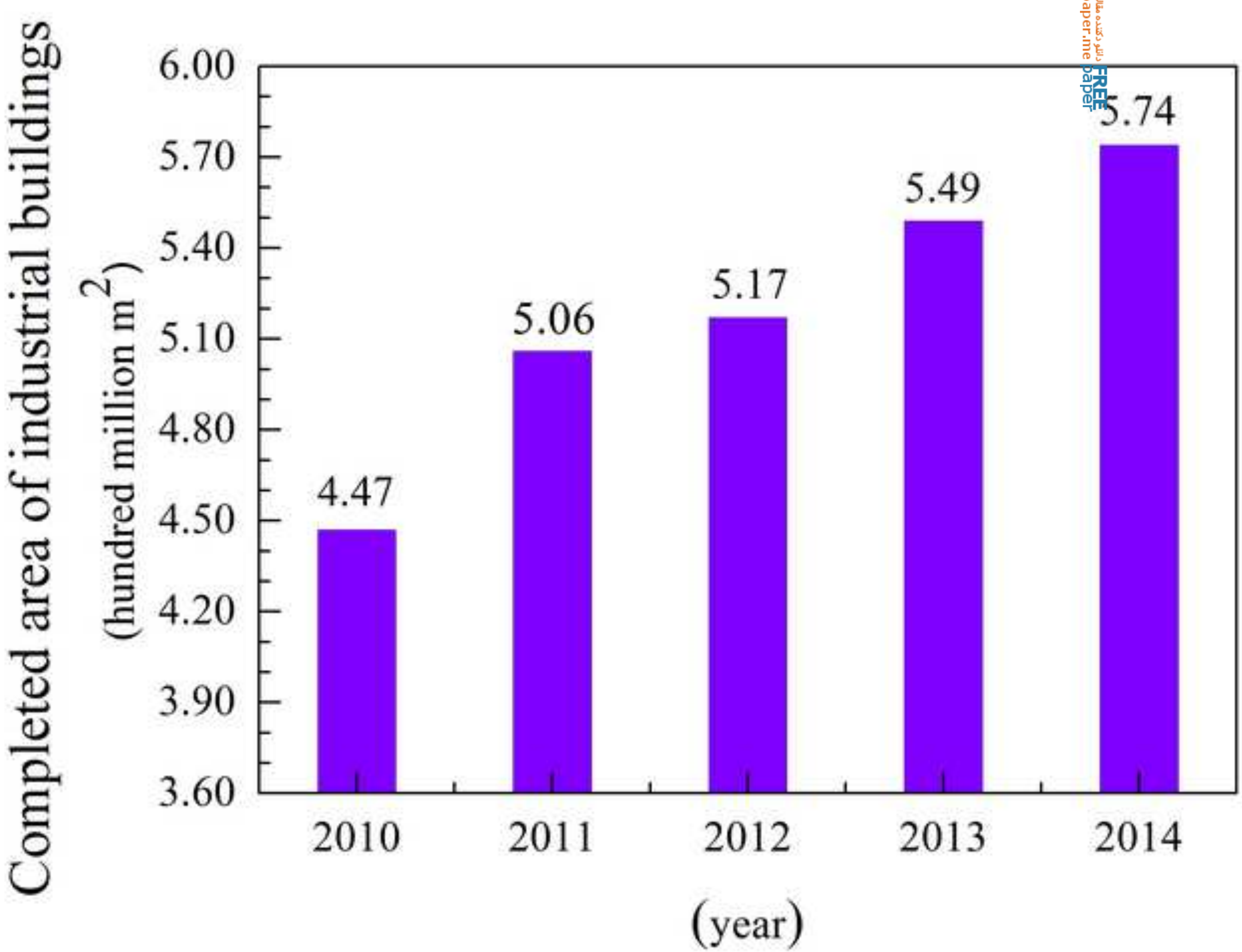

Fig.2-revised

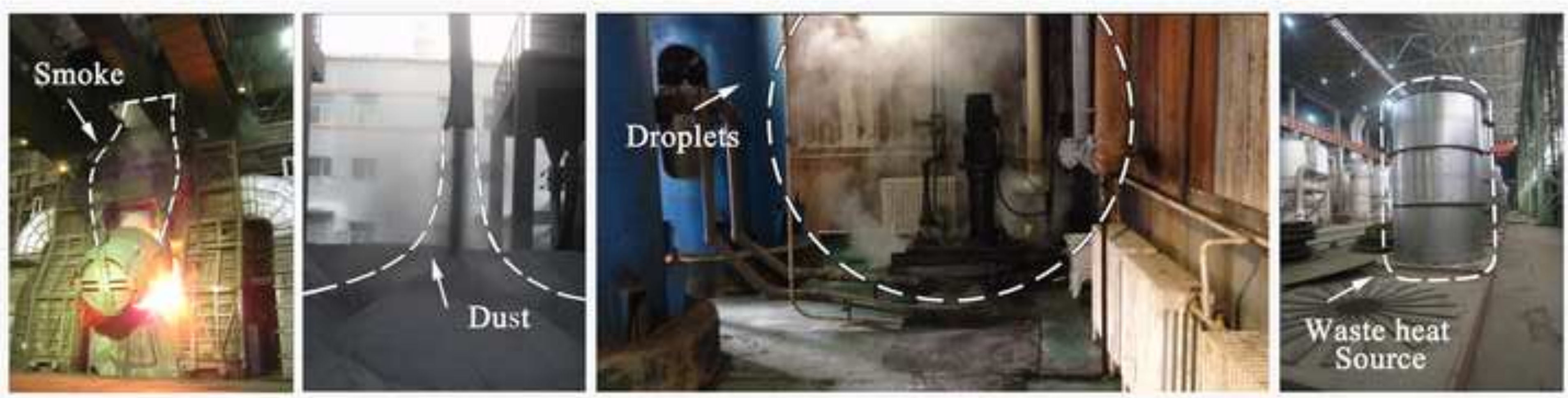

Fig.3-revised

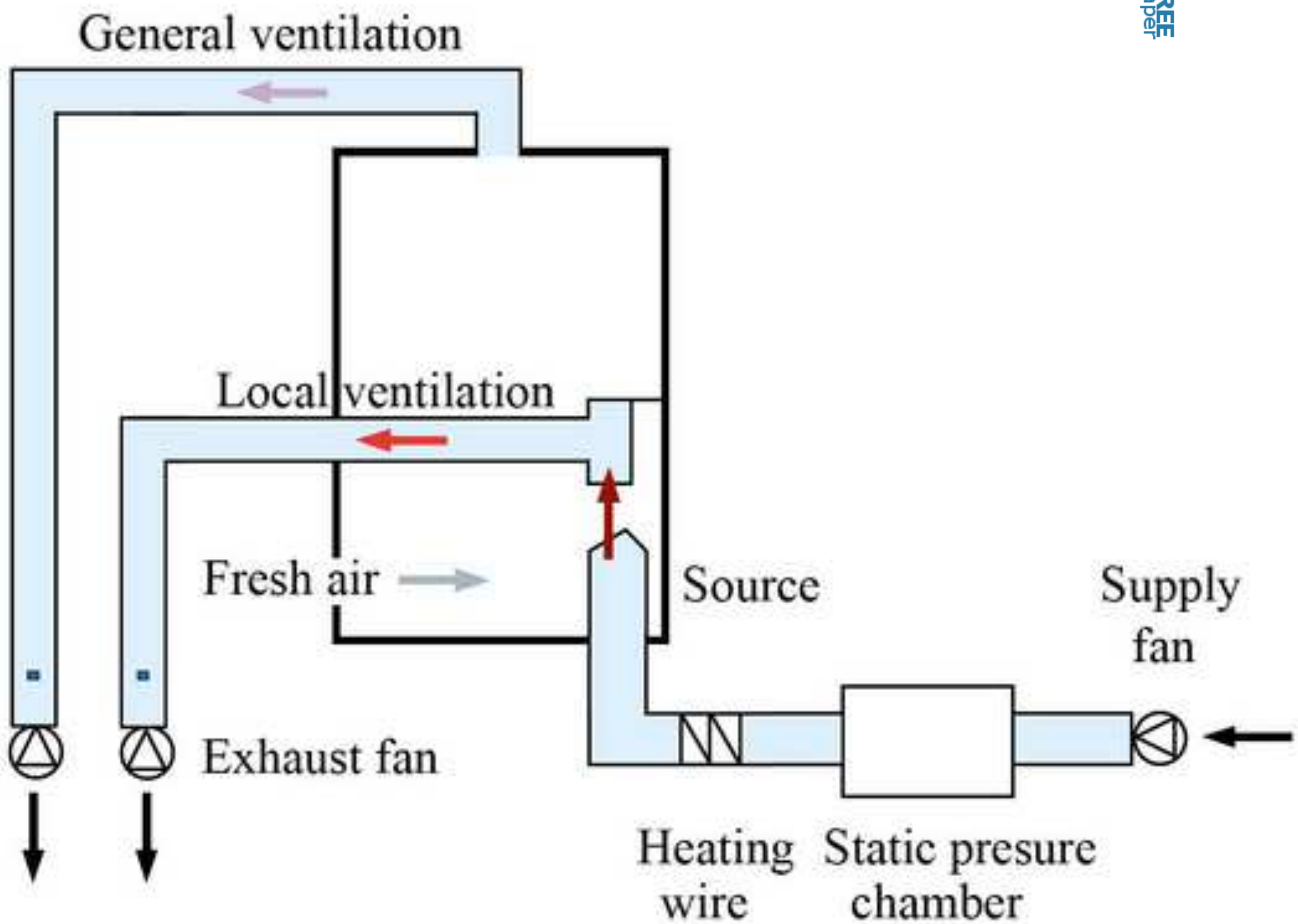

Fig.4-revised

Click here to download high resolution image

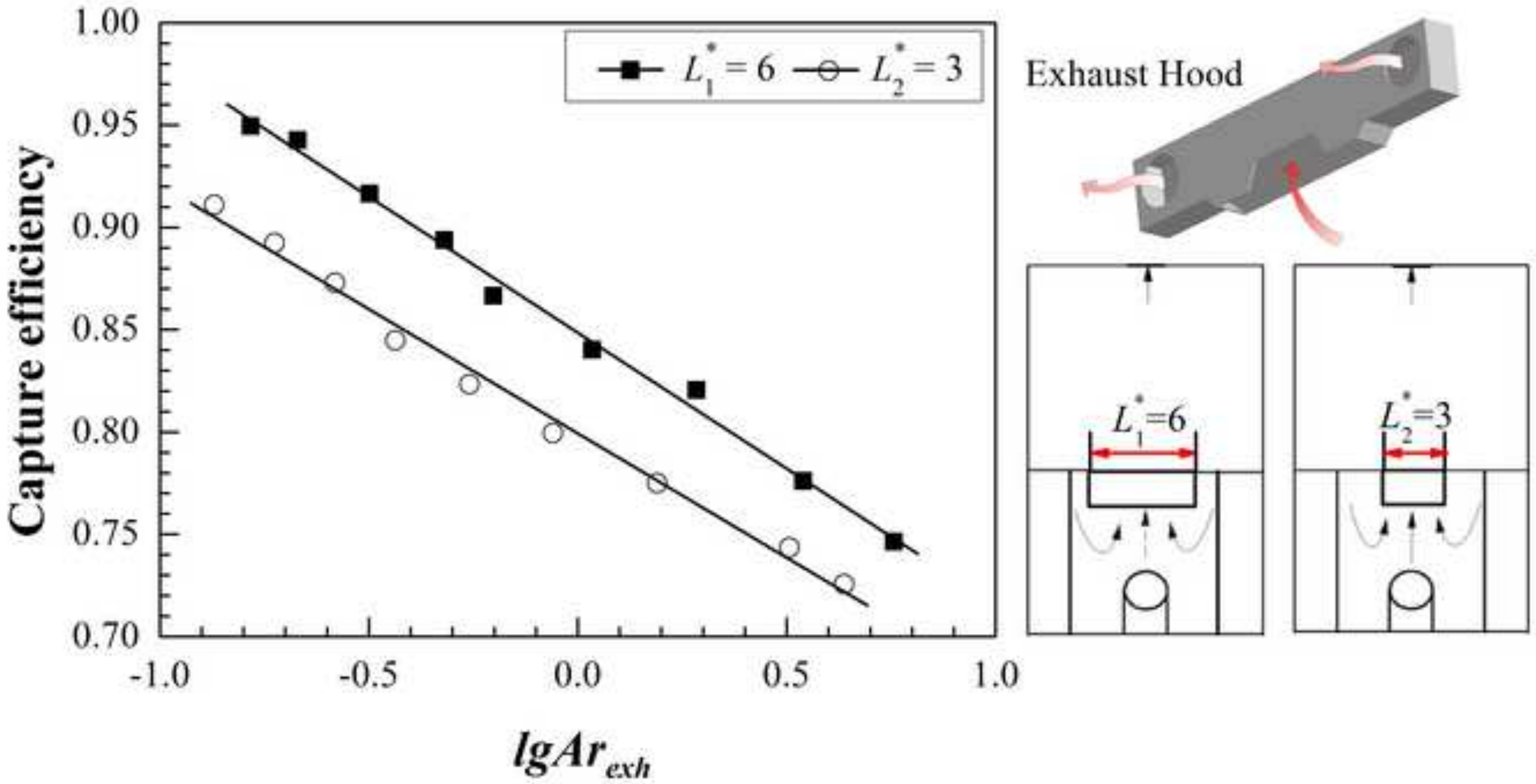

Fig.5-revised

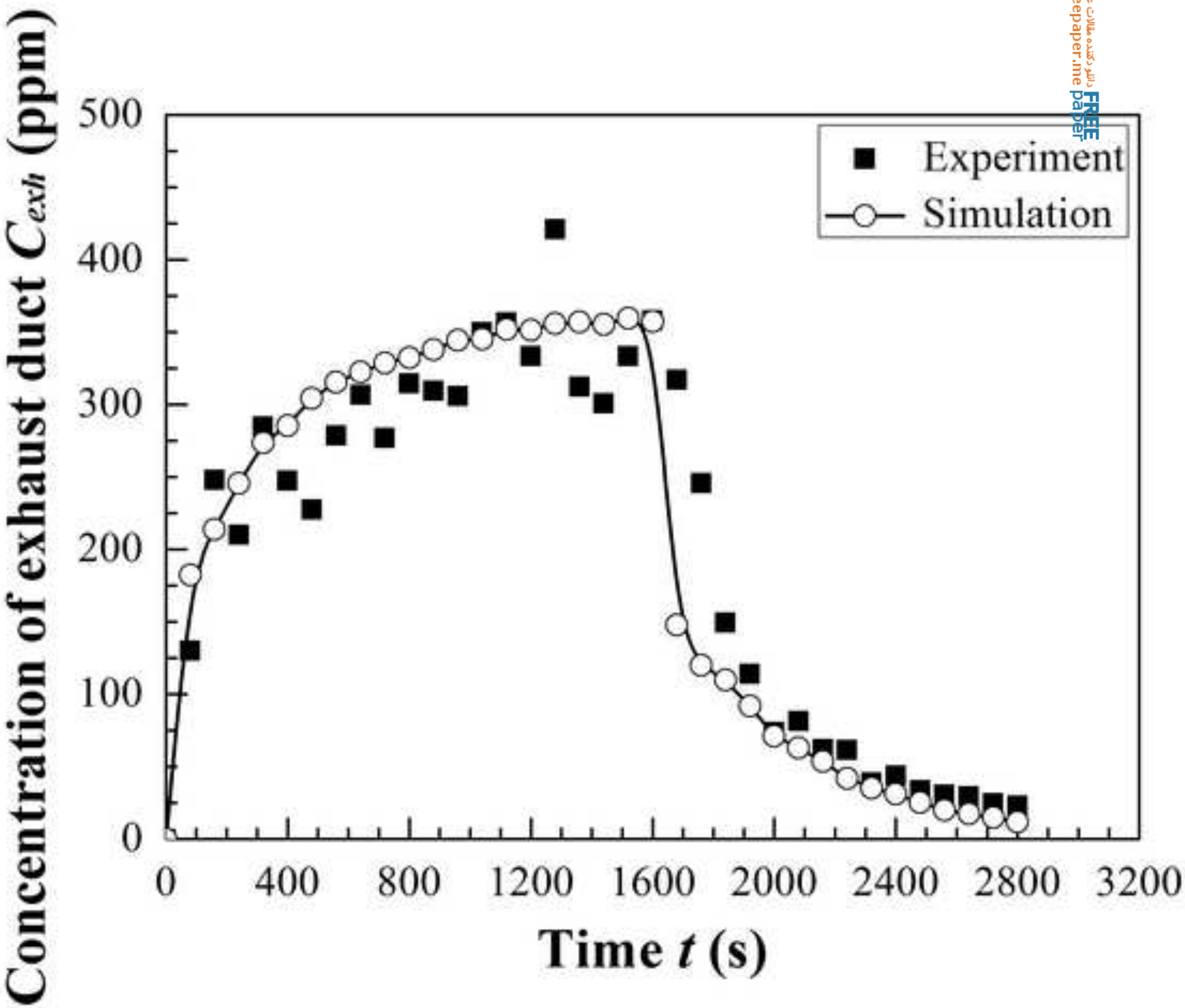

Fig.6 (a)-revised

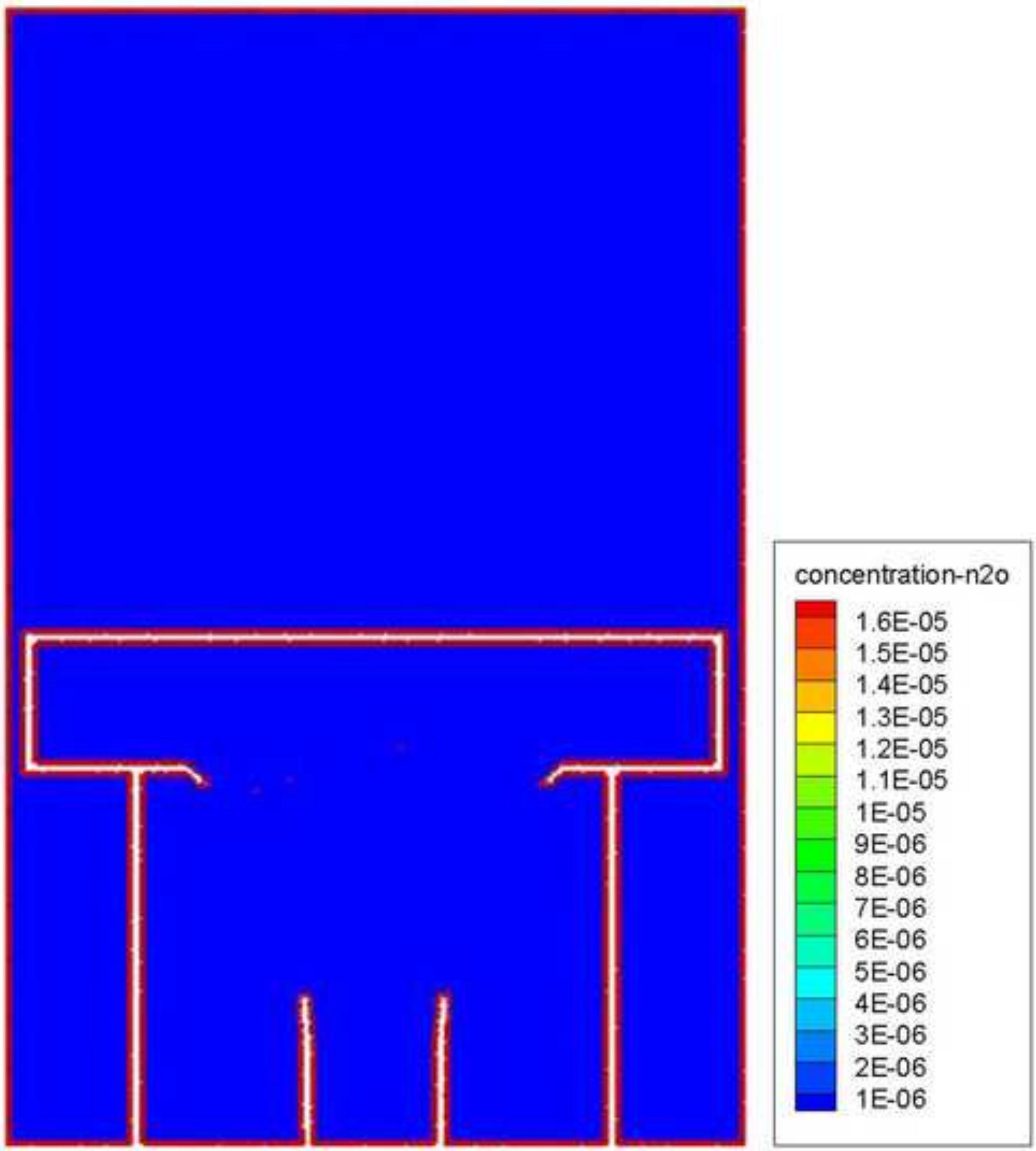

Fig.6 (b)-revised

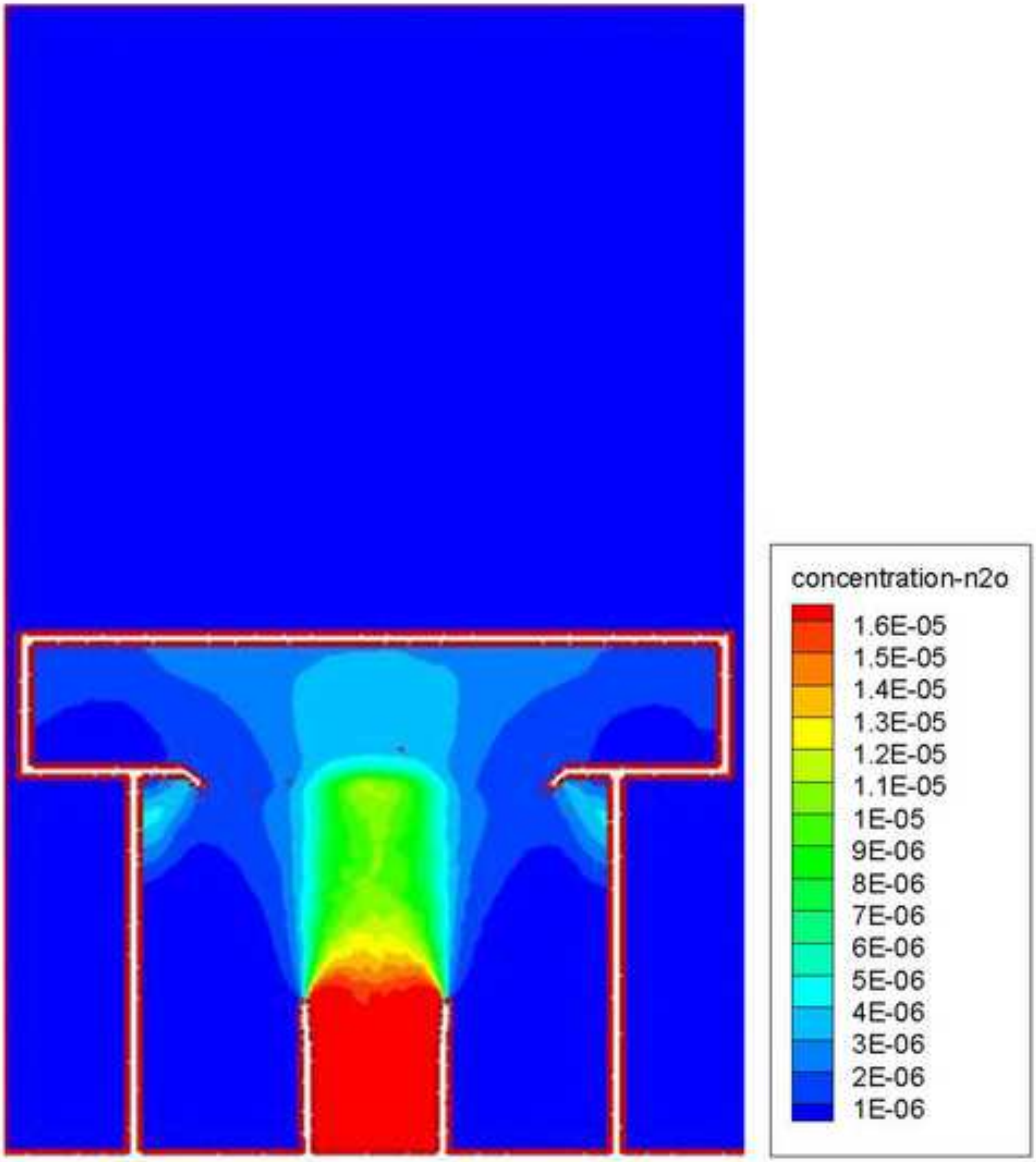

Fig.6 (c)-revised

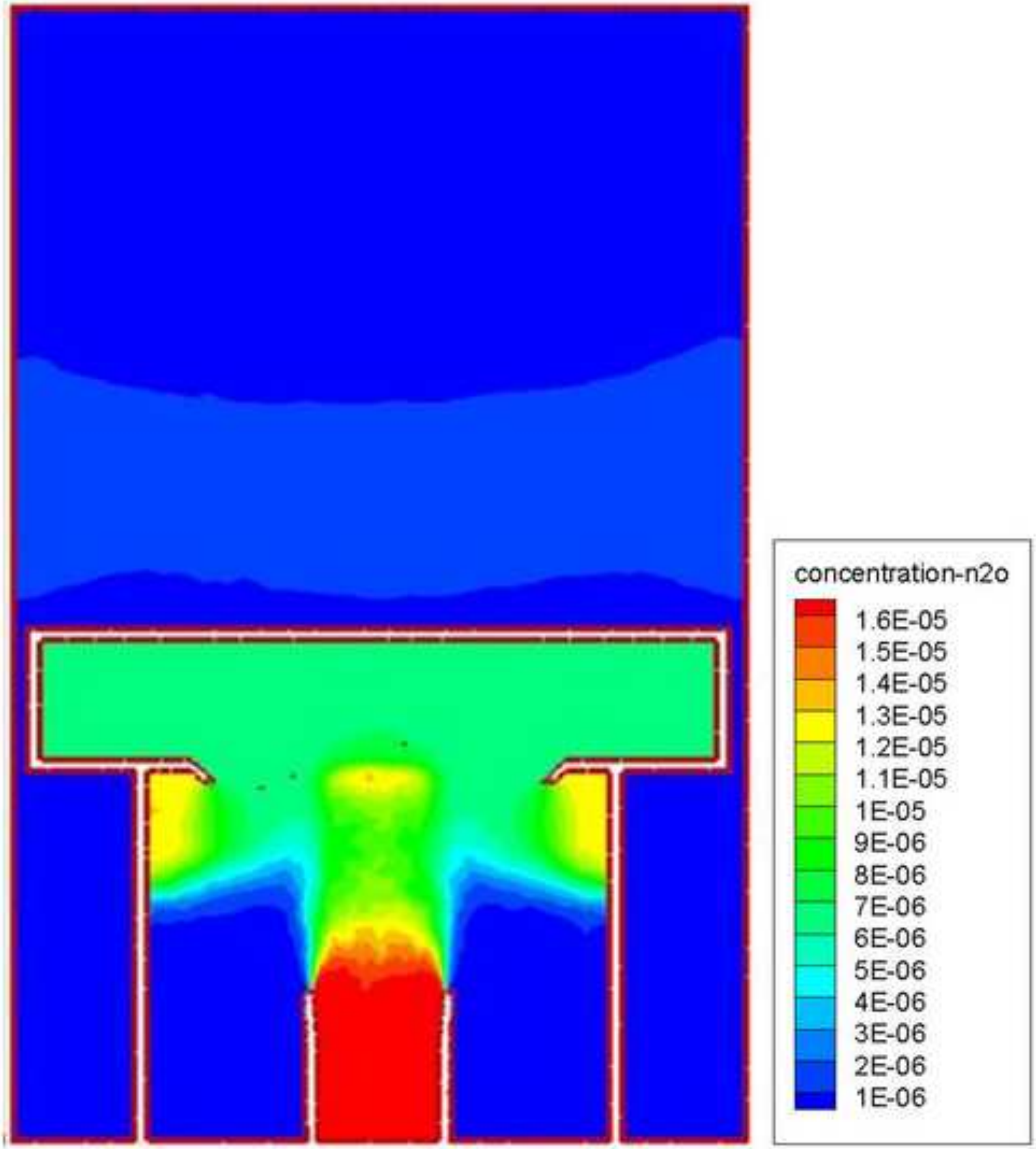

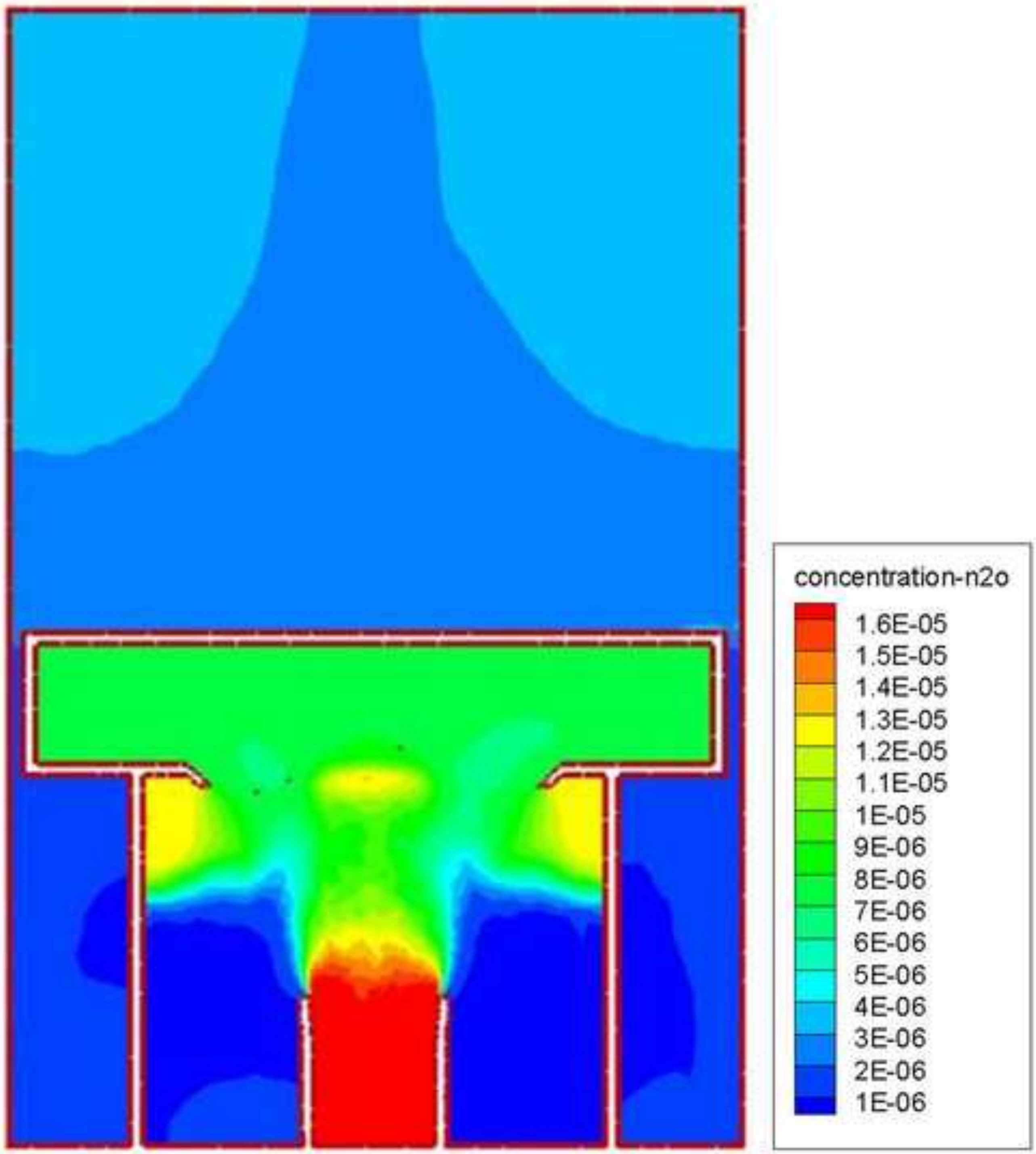
concentration-n2o
1.6E-05
1.5E-05
1.4E-05
1.3E-05
1.2E-05
1.1E-05
1E-05
9E-06
8E-06
7E-06
6E-06
5E-06
4E-06
3E-06
2E-06
1E-06

Fig.6 (e)-revised

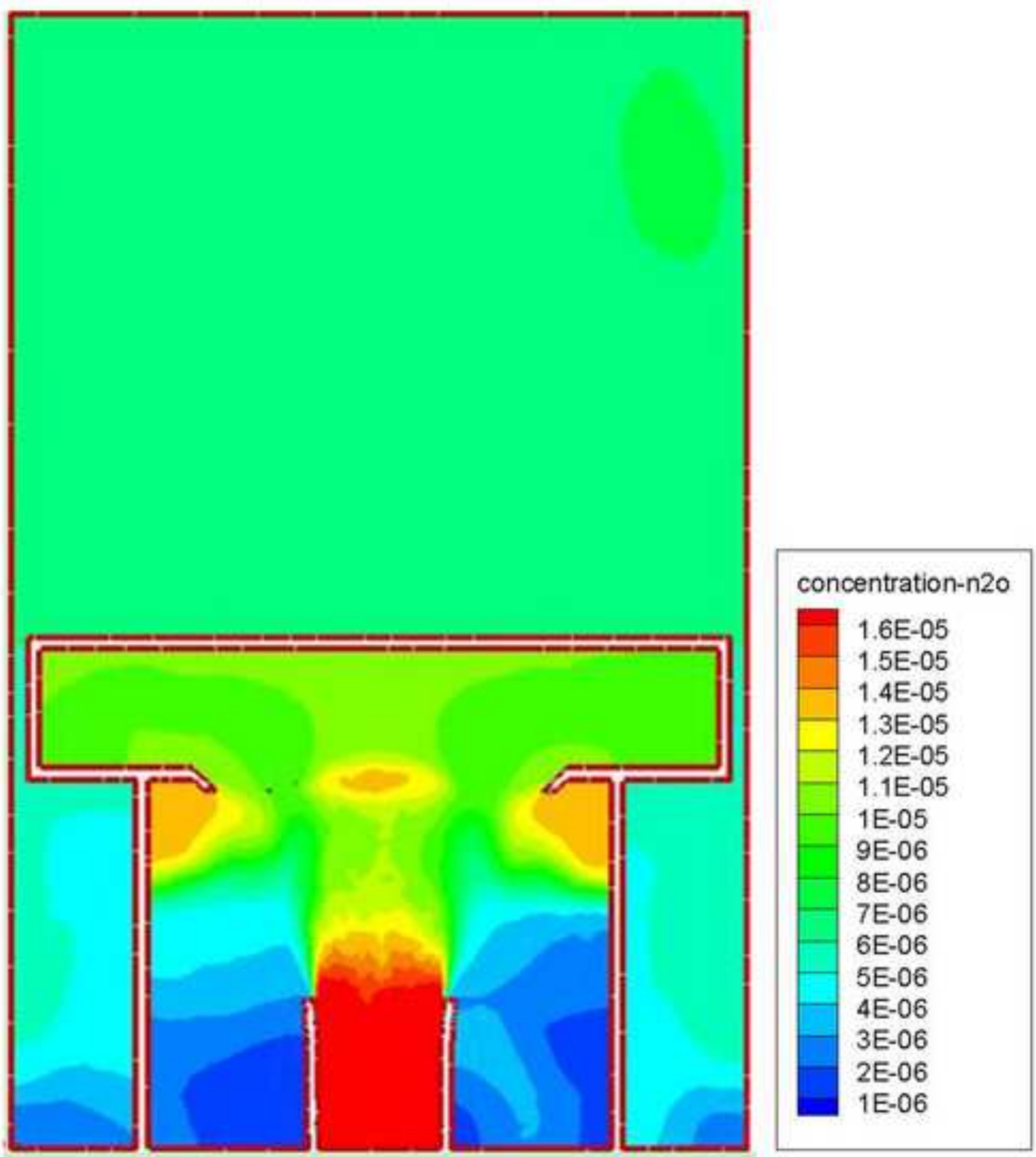

Fig.7-revised

Click here to download high resolution image

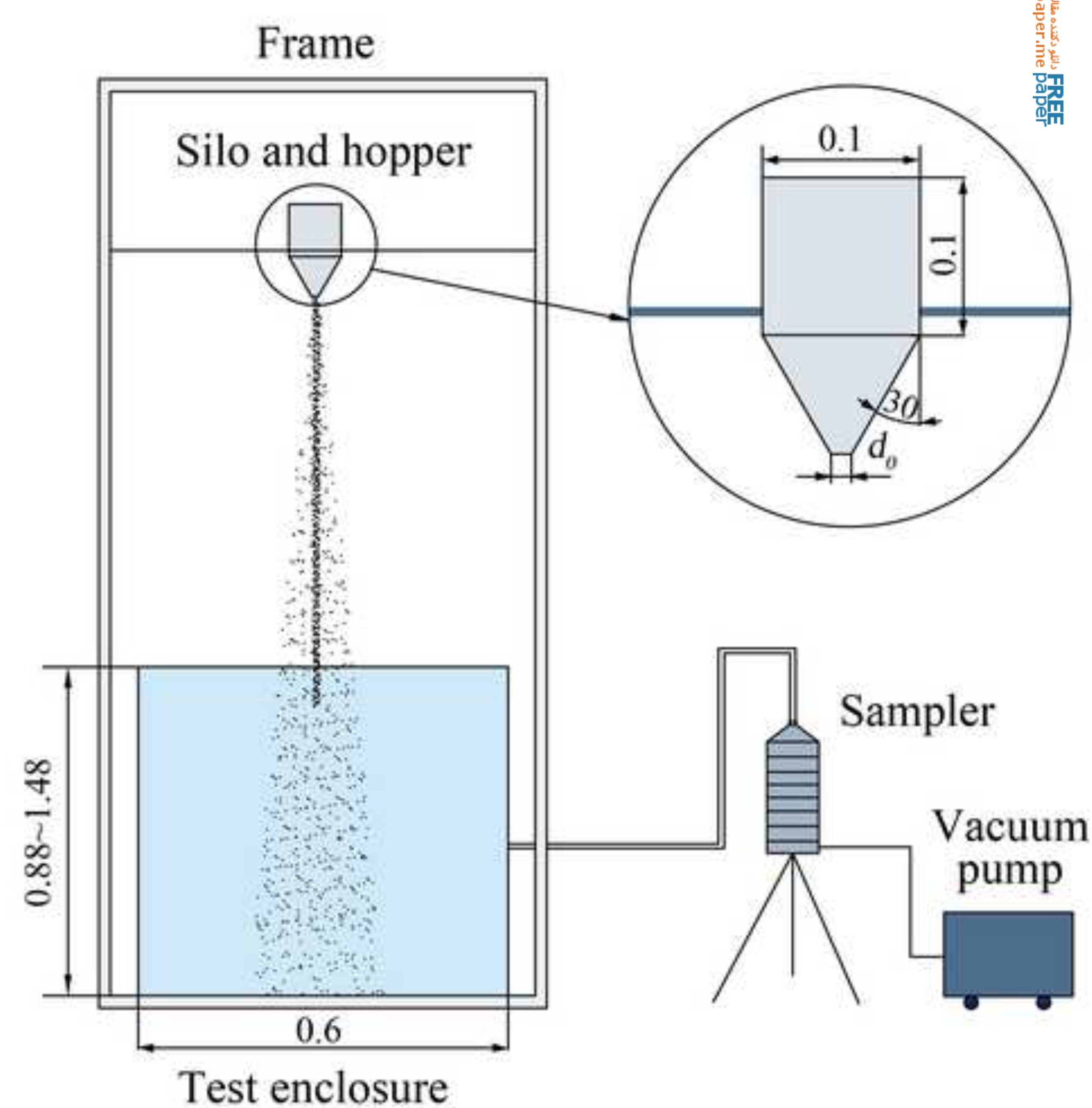

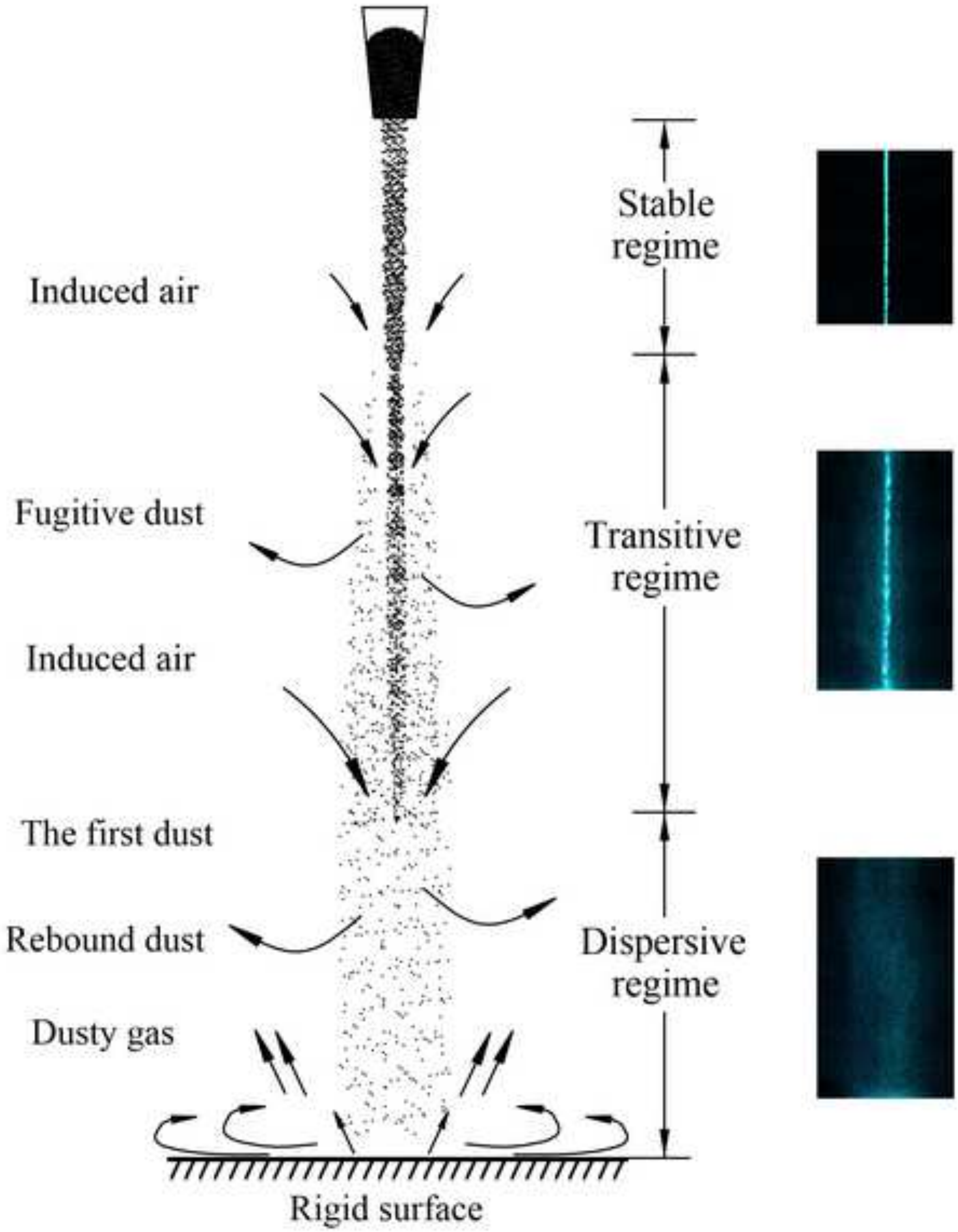
Stable
regime
Induced air
Fugitive dust
Transitive
regime
Induced air
The first dust
Rebound dust
Dispersive
regime
Dusty gas
Rigid surface

Fig.8 (b)-revised

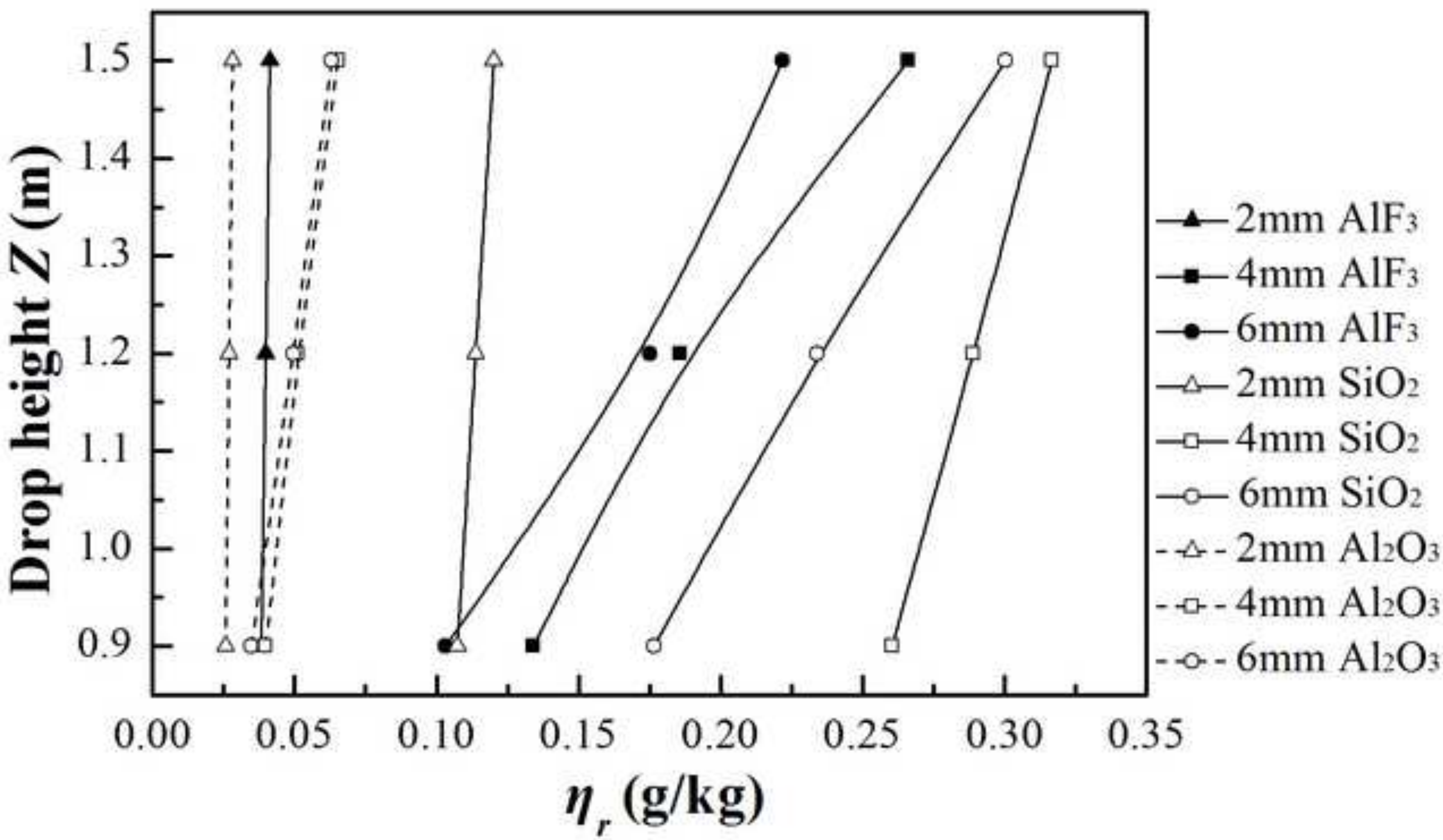

Fig.9-revised

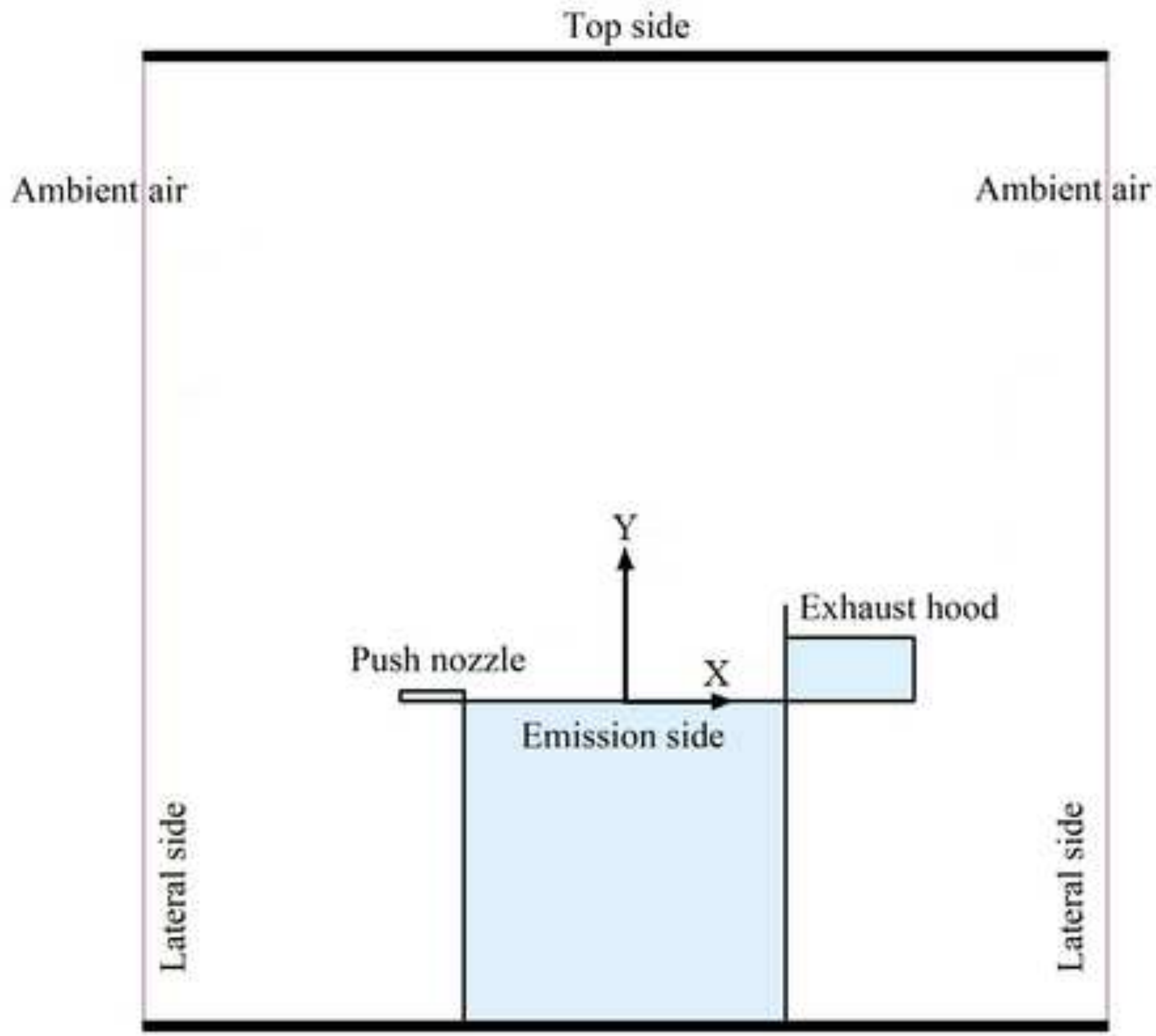

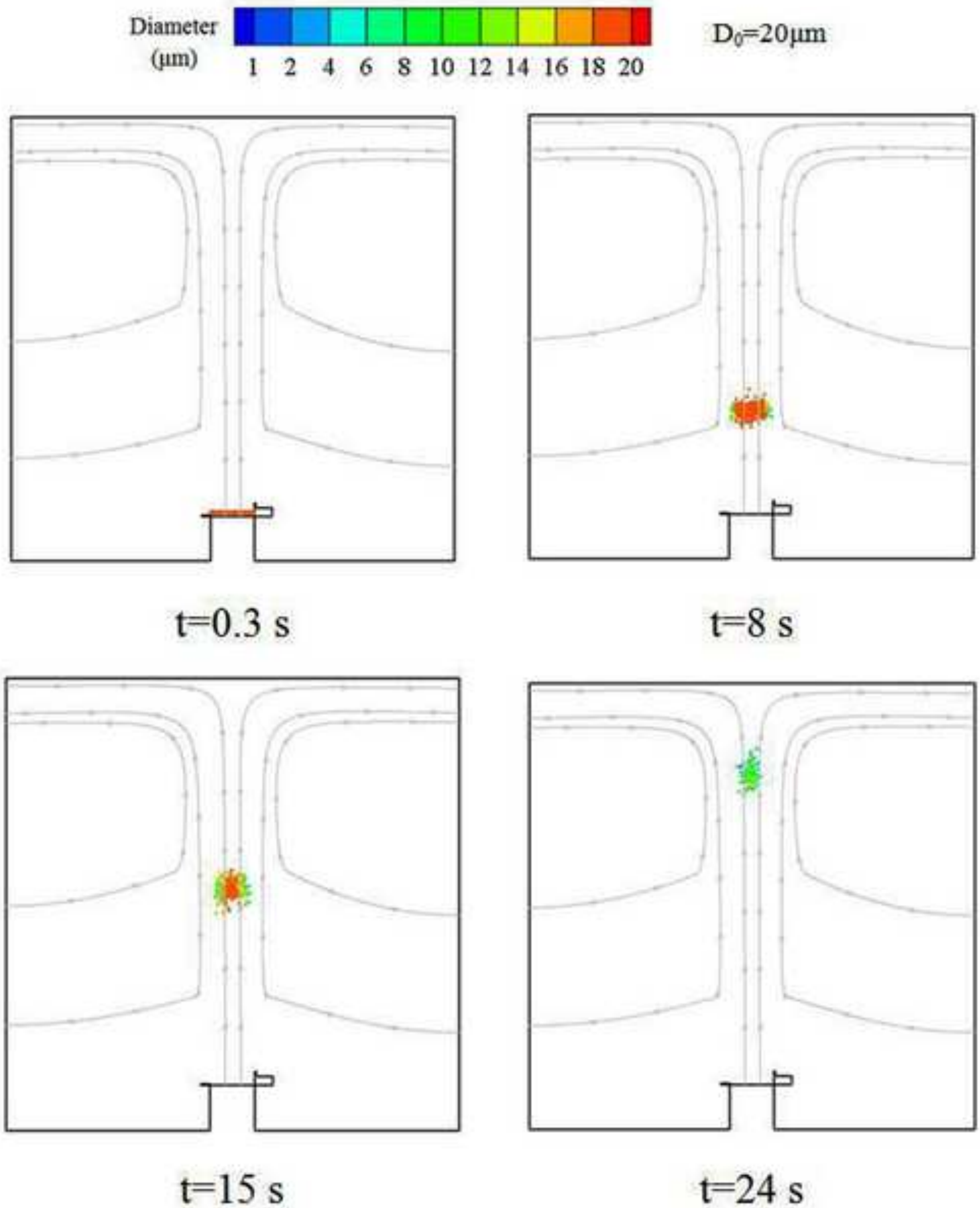
Diameter
(μm)
1 2 4 6 8 10 12 14 16 18 20
D0=20μm
t=0.3 s
t=8 s
t=15 s
t=24 s

Fig.10 (b)-revised

Click here to download high resolution image

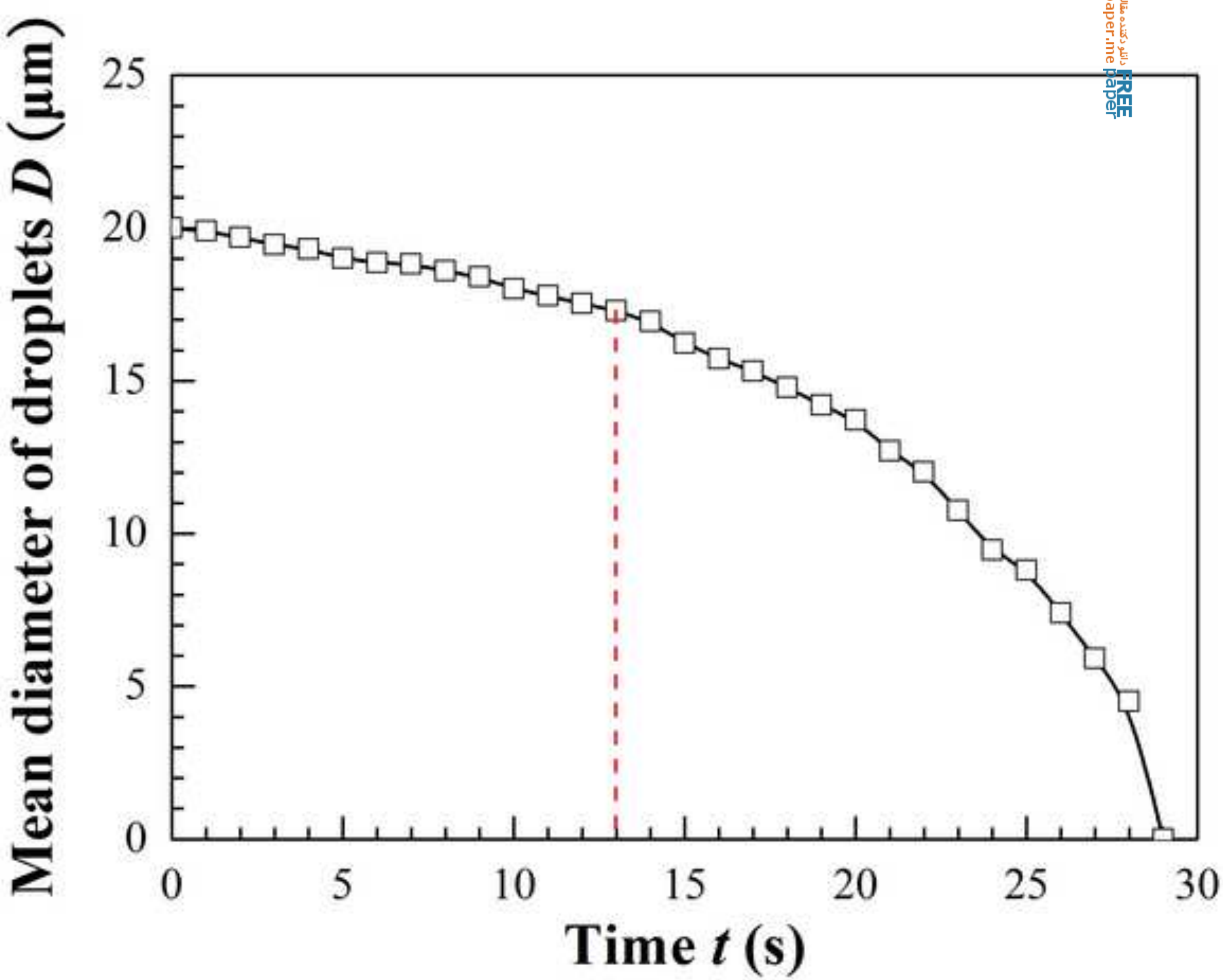

Fig.11 (a)-revised

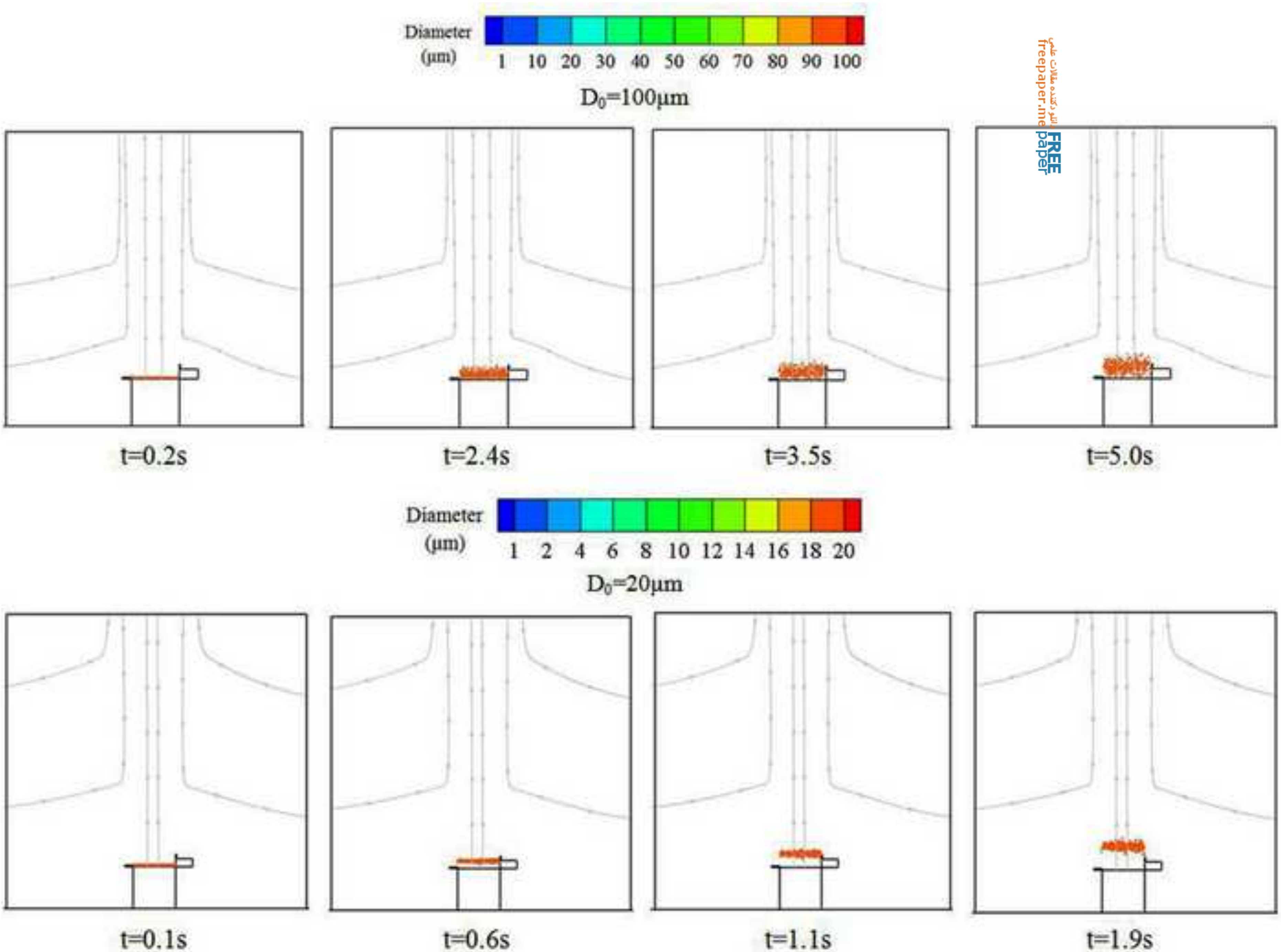

Fig.11 (b)-revised

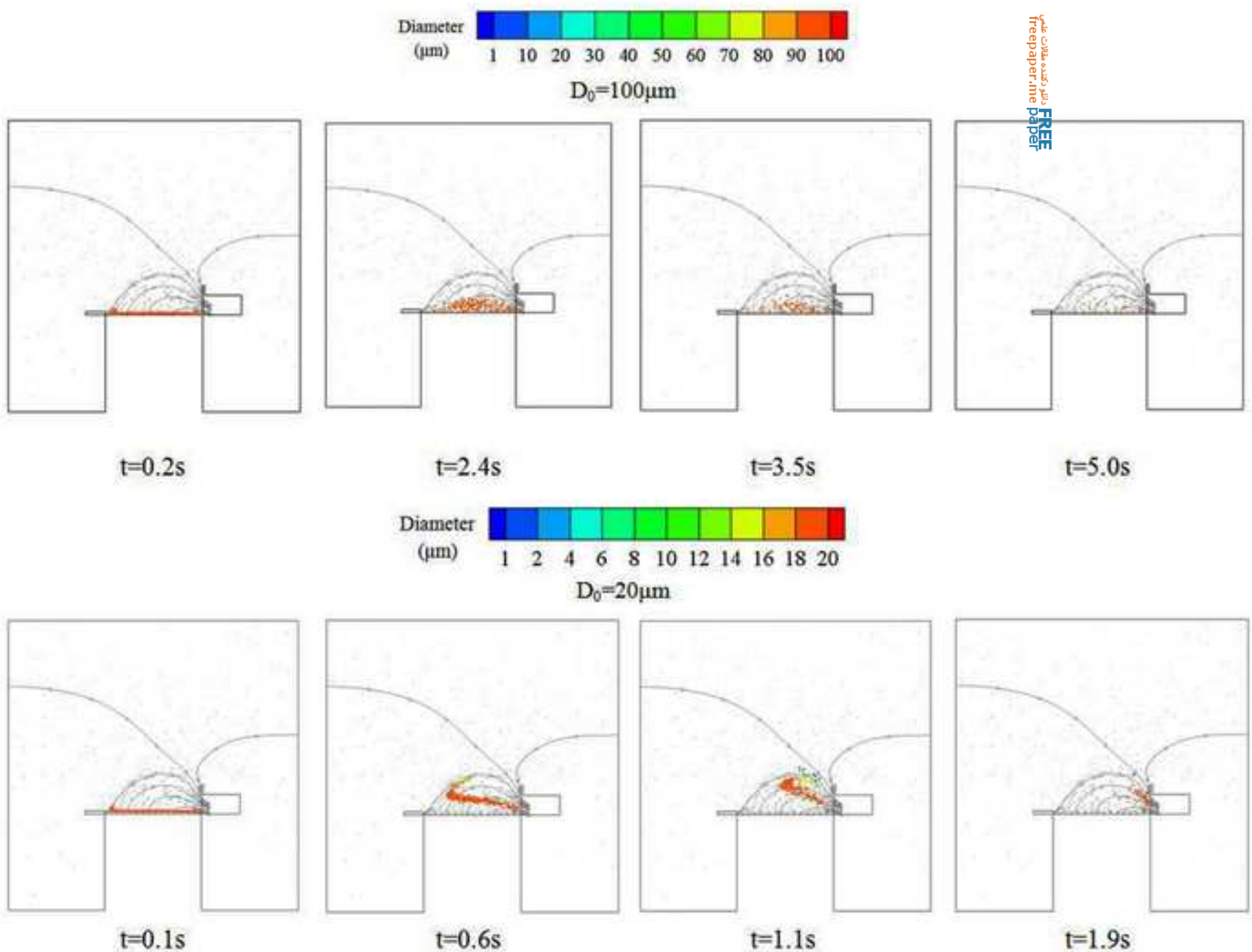

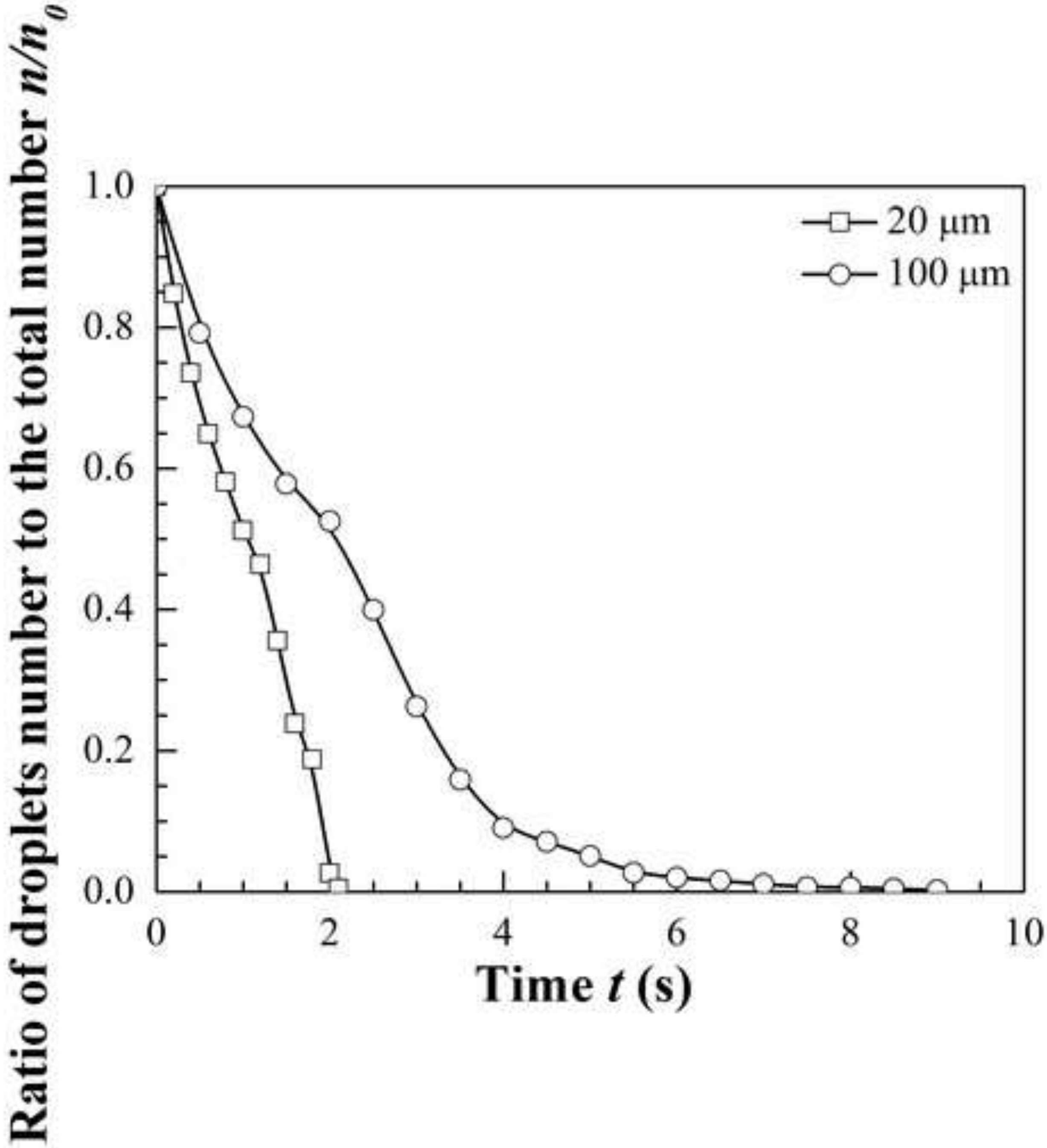
Ratio of droplets number to the total number n/n0
1.0
0.8
0.6
0.4
0.2
0.0
0
2
4
6
8
10
Time t (s)
20 µm
100 µm

Fig.12-revised

Click here to download high resolution image

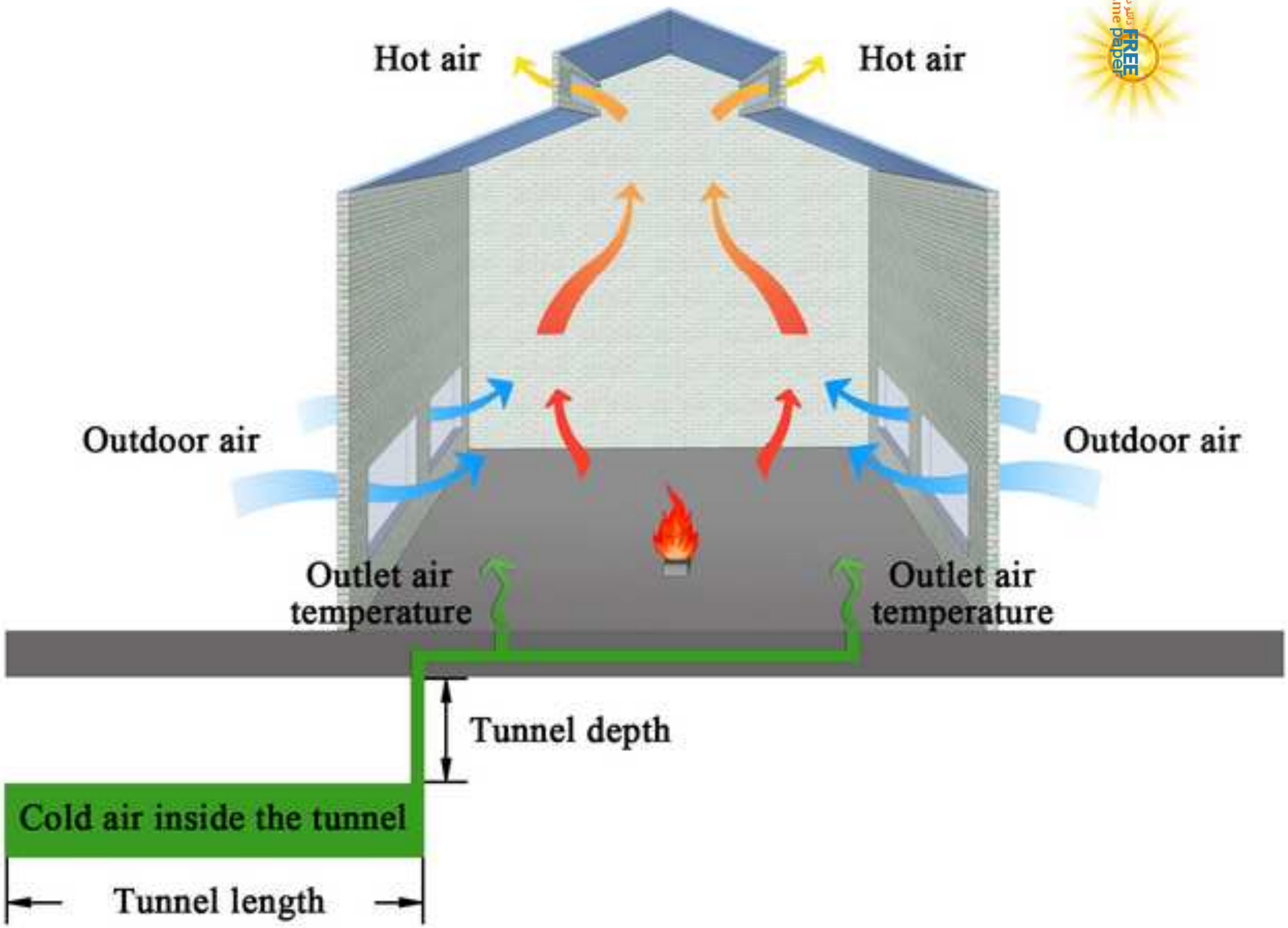

Fig.13 (a)-revised

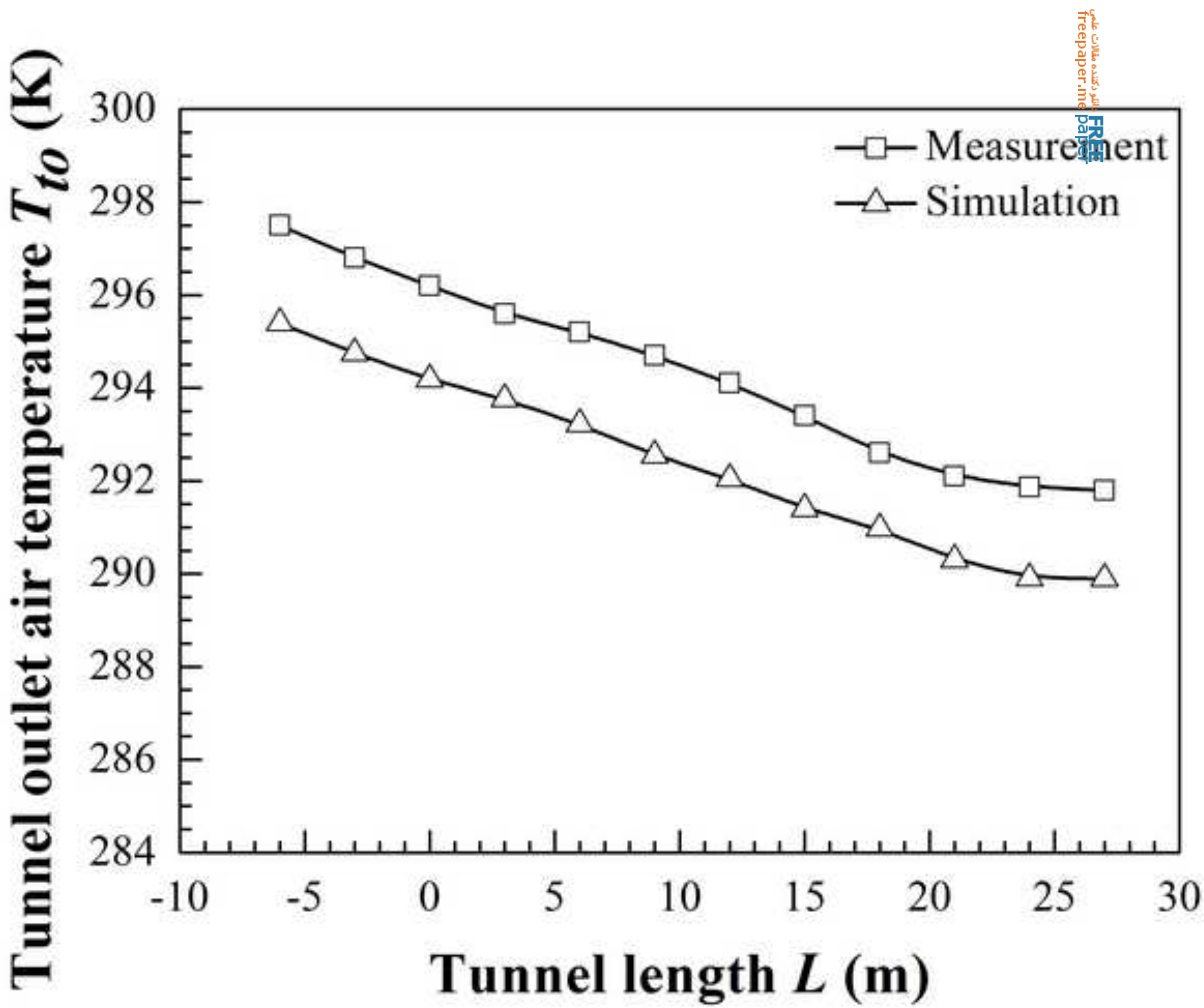

Fig.13 (b)-revised

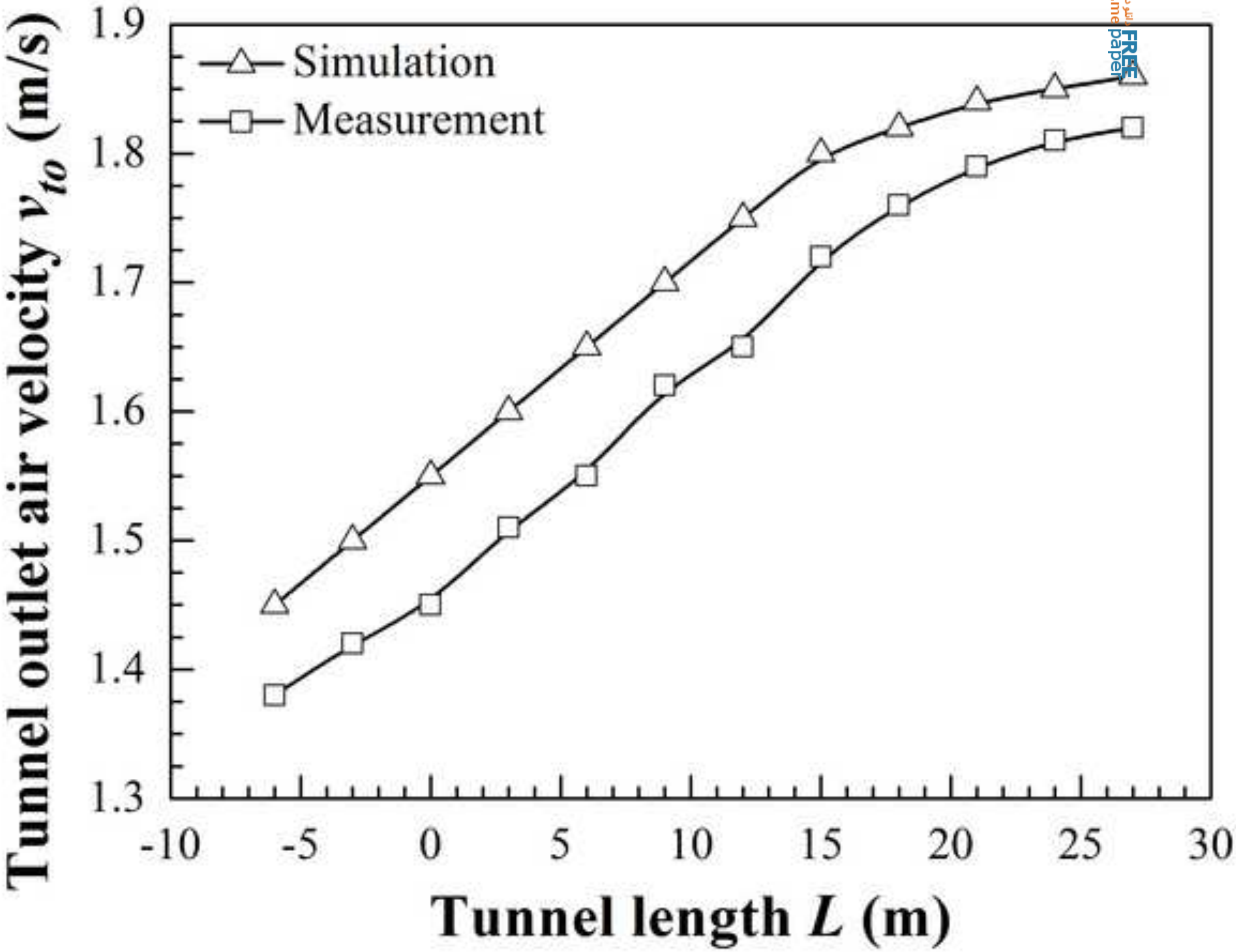

Fig.14 (a)-revised

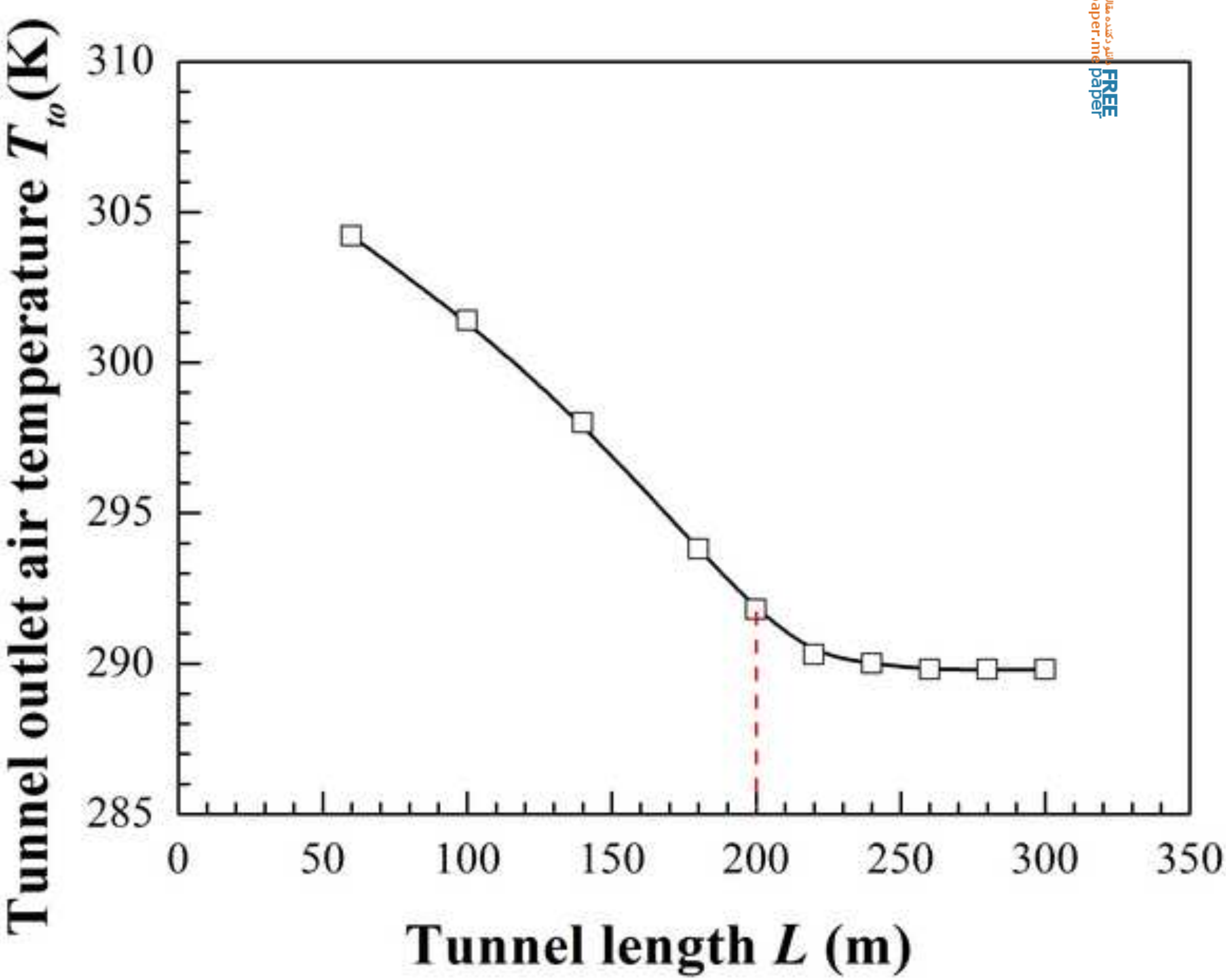

Fig.14 (b)-revised

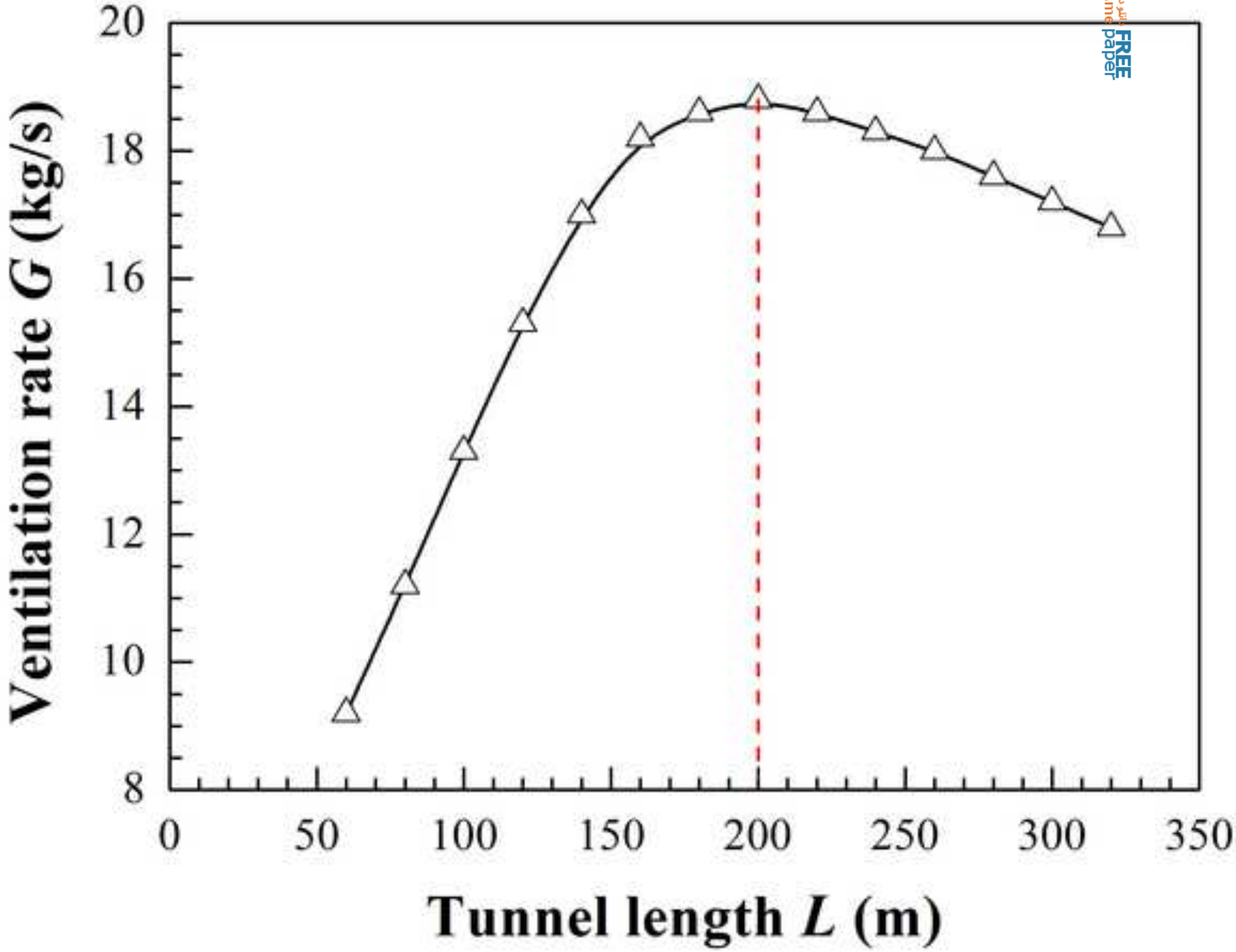

Table 1

Boundary conditions for numerical simulation

Name[8]	Boundary conditions	Details
Source	Velocity inlet	v_s=0.217 m/s, T_s=313.4 K, $C_s(N_2O)$= 360 ppm
Fresh air inlet	Pressure inlet	Gauge pressure P_f=0, T_f=296.7 K
General ventilation outlet	Velocity outlet	v_{outlet} = -0.089 m/s, T_{outlet} =297.9 K
Exhaust duct	Velocity outlet	v_{exh}=0.354 m/s, T_{exh}=299.1 K
Others	Constant wall temperature	Based on experimetal measurements[8]

Table 2

Physical property parameter and dispersity of three materials

Material	ρ_p (kg/m^3)	ρ_b (kg/m^3)	$\overline{d_p}$ (μm)	Percentage of 0~10 μm particles (%)
Al_2O_3	2683.48	1147.61	58.43	2
AlF_3	2951.74	1439.08	53.73	10
SiO_2	2234.43	1109.52	55.19	12